Redescription of *Pelagia benovici* into a new jellyfish genus, *Mawia*, gen. nov., and its phylogenetic position within Pelagiidae (Cnidaria : Scyphozoa : Semaeostomeae)

M. Avian[A,F,*], *A. Ramšak*[B,*], *V. Tirelli*[C], *I. D'Ambra*[C,D] *and A. Malej*[B,E]

[A]Department of Life Science, University of Trieste, Via L. Giorgieri 10, 34127 Trieste, Italy.
[B]National Institute of Biology, Marine Biology Station, Fornače 41, 6330 Piran, Slovenia.
[C]Istituto Nazionale di Oceanografia e di Geofisica Sperimentale – OGS, Oceanographic Section, Via A. Piccard 54, 34151, Trieste, Italy.
[D]Present address: Stazione Zoologica Anton Dohrn, Villa Comunale, 80121 Napoli, Italy.
[E]Present address: M'Aleja, Čevljarska 35, 6000 Koper, Slovenia.
[F]Corresponding author. Email: avian@units.it
[*]M. Avian and A. Ramšak contributed equally to this work.

Abstract. This study provides new and additional data on morphology and a phylogenetic analysis of the recently described species *Pelagia benovici* Piraino, Aglieri, Scorrano & Boero, 2014 from the Northern Adriatic (Mediterranean Sea). Comprehensive morphological analyses of diagnostic characters, of which the most significant are marginal tentacles anatomy, basal pillars, gonad pattern, subgenital ostia and exumbrellar sensory pits, revealed significant differences from the currently known genera *Sanderia*, *Chrysaora* and *Pelagia* in the family Pelagiidae. A phylogenetic analysis of mitochondrial genes (COI, 16S rRNA, 12S rRNA) and nuclear ribosomal genes (28S rRNA, ITS1/ITS2 regions), together with cladistic analysis of morphological characters, positioned *Pelagia benovici* as a sister taxon with *Sanderia malayensis*, and both share a common ancestor with *Chrysaora hysoscella*. *Pelagia benovici* does not share a direct common ancestor with the genus *Pelagia*, and thus we propose it should not belong to this genus. Therefore, a new genus *Mawia*, gen. nov. (Semaeostomeae : Pelagiidae) is described, and *Pelagia benovici* is renamed as *Mawia benovici*, comb, nov.

Additional keywords: Semaeostomeae, Pelagiidae, *Pelagia*, *Mawia benovici*, taxonomy, phylogeny.

Accepted 18 October 2016

Introduction

Exact recognition of a species is one of the basic requirements in ecology and in many related disciplines that rely on an accurate species delimitation derived from systematics. In particular, it is crucial to determine the dynamics and evolution of populations based on the connectivity of evolutionary relevant units (Pante *et al.* 2015*a*). Besides understanding their evolutionary history and relationships, both of which are closely linked with an accurate definition of a species, there are also practical requirements for accurate species identification, such as recognition of invasive jellyfish and the associated risk for humans (Gershwin and Collins 2002 and references therein), or estimation of jellyfish biomass and their ecosystem relevance (Bastian *et al.* 2014). Scyphozoan systematics is complicated owing to complex life cycles, unpredictable appearances, ecological plasticity and also because of the lack of trained taxonomists (Boero 2010; Markmann and Tautz 2005). All of these factors have led to numerous taxonomical re-arrangements in classical books (Mayer 1910; Kramp 1961; Russell 1970; Franc 1993), as well as in current periodic literature (Collins 2002; Marques and Collins 2004; Morandini and Marques 2010).

There have been many rearrangements of the genus *Pelagia* since Mayer's synopsis of the 'Medusae of the World' was published in 1910. Several species in the genus *Pelagia* were proposed by Mayer (1910), but currently only the type species, *Pelagia noctiluca* (Forskål, 1775), is considered a valid species (but see Morandini and Marques 2010: table 1). Moreover, a cladistic analysis of pelagiid species reassigned *Pelagia colorata* Russell, 1964 as *Chrysaora colorata* (Gershwin and Collins 2002). An approach coupling morphological and phylogenetic analyses in scyphozoan systematic can help overcome these difficulties, reveal evolutionary relationships, and possibly facilitate the redescription of taxa (Marques and Collins 2004; Dawson 2005*a*, 2005*b*). However, Gershwin and Collins (2002) pointed out that identifying a suitable outgroup for a pelagiid phylogenetic analysis is very difficult, and for this reason it is particularly hard to establish the true direction of character changes.

The description of a new species, *Pelagia benovici* Piraino, Aglieri, Scorrano & Boero, 2014 (Piraino *et al.* 2014), from the northern Adriatic Sea opened some questions. These medusae were classified within the genus *Pelagia* according to morphological features (shape and colouration of umbrella; shape and distribution of cnidocyst warts; thickness of mesoglea; shape and number of marginal lappets; morphology and number of rhopalia; number, arrangement and relative length of tentacles; presence or absence of muscular folds in tentacle sections; relative length and shape of manubrium and oral arms; shape and arrangement of radial septa in the gastrovascular cavity; number and shape of gonads; cnidocyst types and sizes) and phylogenetic analysis. In particular, molecular analysis of the COI gene revealed *Pelagia benovici* as a separate group from *Pelagia noctiluca*, while the analysis of 28S rRNA led authors to suggest incomplete lineage sorting or hybridisation events among *Pelagia benovici* and *Pelagia noctiluca* (Piraino *et al.* 2014). This evidence causes an uncertain phylogenetic relationship between *Pelagia benovici* and *Pelagia noctiluca*. We collected specimens of *Pelagia benovici* in the northern Adriatic Sea from September 2013 to August 2014, and here provide new and additional morphological data and a phylogenetic analysis (nuclear 28S rRNA, ITS1/ITS2 regions; mitochondrial genes COI, 16S rRNA and 12S rRNA) of these scyphomedusae. A comprehensive and detailed redescription of *Pelagia benovici* is presented, and we show that the morphological and molecular characteristics of this species require the creation of a new genus.

Material and methods

The Latin name *Pelagia benovici* will be used in our text until we provide a description of the new genus in the results section.

Sampling and observations

We collected, as by-catch, hundreds of specimens of *Pelagia benovici* that were at that time still undetermined (Figs 1, 2*a*, *b*) during a small pelagic acoustic survey carried out in the Adriatic Sea on 6 September 2013 at a station located ~16 nm off shore from the Po delta. Despite the large number of specimens collected in the trawling net, we did not observe these medusae in the surface water, and did not find the species again during the following 2 weeks. After this first finding, no large aggregations were observed, but several individuals were noted and sampled in different locations in the Gulf of Trieste from late November 2013 to March 2014 (Figs 1, 2 and Table 1). One specimen was seen and photographed in the Venice Lagoon on 24 December 2013 (Bastianini, pers. communication, Supplementary Material 1). Two specimens were again collected on 31 August 2014 offshore from the Po delta, in the same area of the September 2013 samplings (Fig. 1, Table 1).

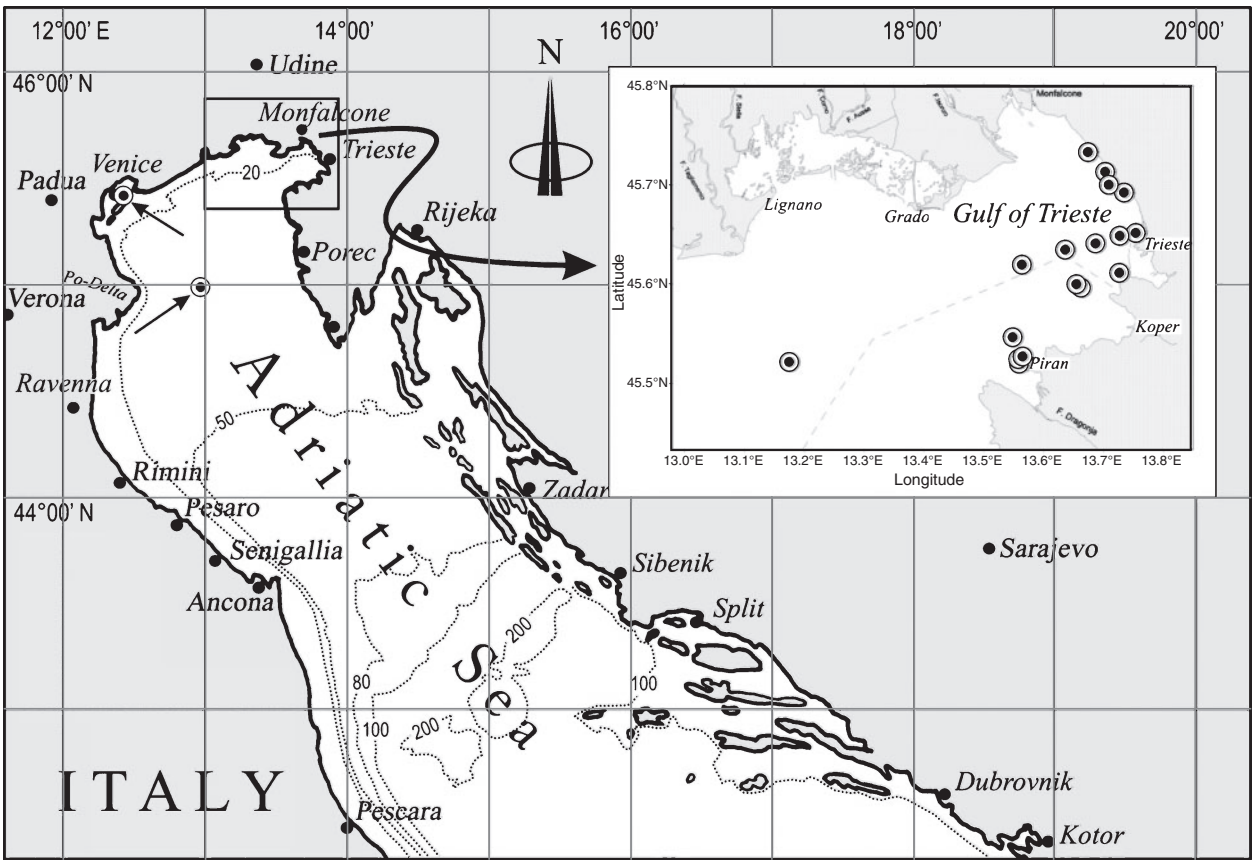

Fig. 1. *Mawia benovici*, map of the sampling and observation sites (September 2013–March 2014).

Fig. 2. *Mawia benovici*, (*a*) and (*b*) collected during the small pelagic ecosurvey of 6 September 2013; (*c*) a lateral view of a jellyfish in the Bay of Piran, 5 February 2005. Well evident is the lack of colouration of the tentacles and oral arms; (*d*) picture taken near the shore in the Bay of Piran, 20 November 2004, with an adult specimen together with *Pelagia noctiluca* specimens. The arrow indicates the dark pink–purple colouration of the gonads. Scale bars = 1 cm.

Specimens were collected with a sampling bucket or with a hand net and immediately transported to the laboratory. They were photographed under a Leica Microsystems M205C stereomicroscope, then preserved in a buffered 4% formaldehyde–saltwater solution. Fifty-three specimens were collected on 4 December 2013, and their tissue samples were immediately preserved in 96% ethanol for molecular and phylogenetic analysis. The dates and location of observations and sampling are presented in Table 1 and Fig. 1. In light of these recent findings, old samples collected and preserved in formalin in summer–autumn 2004 and winter 2005 in the Gulf of Trieste and pictures taken near the shore of Piran (Slovenia) during winter 2004–05, were reexamined (Fig. 2*c*, *d*).

In order to obtain additional comparative data on pelagiid morphology, the following specimens were analysed: *Sanderia malayensis* Goette, 1886 (one specimen from Kamo aquarium, Japan, and one from Schönbrunner Tiergarten, Wien, Austria); *Chrysaora fuscescens* Brandt, 1835 (one specimen from Schönbrunner Tiergarten, Wien, Austria); *C. hysoscella* (Linnaeus, 1767) (several specimens collected from the Gulf of Trieste in February–March 2014); *C. lactea* Eschscholtz, 1829 (two specimens from the Departamento de Zoologia, Instituto de Biociências, Sao Paulo, Brazil); *C. pacifica* (Goette, 1886) (two specimens from Shimanoseki, the strait between Honshu and Kyushu Islands, collected in March 2015); *C. plocamia* (Lesson, 1830) (one specimen from the Departamento de Zoologia, Instituto de Biociências, Sao Paulo, Brasil); and several specimens of *Pelagia noctiluca* (Forskål, 1775) (from the Strait of Messina, Italy, collected in February 2014). Moreover, six specimens of *Chrysaora hysoscella* and additional specimens of *Pelagia noctiluca* from the Western and Eastern Mediterranean Sea were studied for phylogenetic inference.

Morphological analysis

Morphology was examined on the living and fixed specimens collected in the Gulf of Trieste (Table 1) and compared with the holotype and paratype I of *Pelagia benovici* deposited in the Collection of the Museum of Adriatic Zoology Giuseppe Olivi (Palazzo Grassi, Chioggia, Padova University). Morphometric measurements were made on six adult specimens of *Pelagia benovici* (four caught in summer–winter 2013, two in June and November 2004) preserved in formaldehyde. All morphometric examinations were performed on specimens taken from the liquid and gently stretched out in a Petri dish. Measurements were performed using a Leica Microsystems M205C Stereomicroscope, or a scanner (Epson expression 1600 pro) equipped with a waterproof container, through Image Pro Plus 4.1 and Adobe Photoshop Elements 13 software. Twenty-eight morphological–morphometric parameters were considered (Fig. 3). Morphometric data normalised as feature/umbrellar diameter ratios are reported in Supplementary Material 2.

Table 1. Observation and sampling of *Mawia benovici* in the northern Adriatic Sea with notes on analysis used in this study: (1) morphological analysis; (2) phylogenetic analysis; and (3) photographs

Date of observation	Latitude (N)	Longitude (E)	Number of specimens	Analysis performed in this study
28 Jun. 2004	45.65	13.74	1	1
19 Nov. 2004	45.00	12.92	Several	
20 Nov. 2004	45.53	13.57	Several	3
5 Feb. 2005	45.55	13.55	Several	
6 Sept. 2013	45.00	12.92	>100	3
29 Nov. 2013	45.52	13.18	14	3
29 Nov. 2013	45.73	13.68	1	1
4 Dec. 2013	45.52	13.57	53	2,3
6 Dec. 2013	45.69	13.74	1	1
6 Dec. 2013	45.65	13.73	1	
6 Dec. 2013	45.64	13.64	1	
16 Dec. 2013	45.73	13.68	1	1
17 Dec. 2013	45.64	13.68	1	
17 Dec. 2013	45.61	13.72	1	
17 Dec. 2013	45.70	13.71	1	
17 Dec. 2013	45.59	13.66	99	
24 Dec. 2013	45.44	12.37	1	
10 Jan. 2014	45.62	13.57	2	
22 Jan. 2014	45.71	13.71	1	1
14 Feb. 2014	45.55	13.55	1	
25 Feb. 2014	45.59	13.66	7	
2 Mar. 2014	45.65	13.74	1	
31 Aug. 2014	45.12	12.98	2	

In order to analyse the morphology and morphometry of the sensory pit, samples of rhopalar umbrellar margin were excised from *Sanderia malayensis*, *Chrysaora hysoscella*, *Pelagia benovici* and *P. noctiluca* specimens, stained with a 1% aqueous solution of methylene blue to contrast the epidermal layer and observed both on exumbrellar and lateral views. Measurements are expressed as *length/maximum depth ratio* (LM ratio) and *asymmetry ratio* (AS ratio), which we defined as the ratio between the drift of the point of maximal pit's depth (md in Fig. 8*c*) towards the sensory pit's distal margin (asd in Fig. 8*c*), and towards the sensory pit's proximal margin (asp in Fig. 8*c*), with a value <1 if the maximal depth is shifted towards the distal margin, >1 if the opposite (scheme of asymmetry ratio is presented in Supplementary Material 3).

Histology of gonads and tentacles were compared among *S. malayensis*, *C. fuscescens*, *C. hysoscella*, *C. lactea*, *C. pacifica*, *C. plocamia*, *P. benovici* and *P. noctiluca*. Small pieces of gonads and tentacles were excised from the formaldehyde-preserved specimens, washed in filtered seawater, and re-fixed in 2% glutaraldehyde–seawater solution (pH = 7.2), again washed in filtered seawater and post-fixed in a 1% OsO_4 seawater solution. Samples were dehydrated in an ascending series of ethanol, then treated in propylene oxide and embedded in Derr 372–732 media. Semi-thin sections were obtained with a Leica Ultracut UCT Ultramicrotome, stained with toluidine blue, and observed under a light microscope (Olympus BX50 or Nikon ECLIPSE E-800 with a DXM 1200 camera).

A cnidome analysis was performed on two fresh specimens of *Pelagia benovici*. Tentacles, oral arms, gastric cirri and portions of exumbrellar warts were excised and put consecutively into a 1M glycerol solution in distilled water started at 0°C to finally at 4°C, left to macerate, and then homogenised. Macerate was filtered through a 500-µm mesh net, centrifuged twice at 5°C for 15 min at 304*g* with an Eppendorf Centrifuge 5804R, and the pellet was resuspended in distilled water. The cnidome was investigated under light microscopy as described above, and scanning electron micrographs (SEM) were made with a Leica 430i Scanning Electron Microscope. Terminology used to describe cnidome follows Watson and Wood (1988), with nematocyst taxonomy based on Mariscal (1974), Östman and Hydman (1997) and Östman (2000).

DNA extraction, PCR amplification and sequencing

DNA was extracted from preserved gonadal tissue samples using Kapa Express Extract (KapaBiosystems) and an E.Z.N.A. Mollusc DNA Kit (OMEGA Bio-Tek). Part of nuclear gene 28S rRNA and ITS1/ITS2 interspacer regions were amplified, as well as parts of three genes from mitochondrial DNA (COI, 16S and 12S). The 28S rRNA was amplified with primers 28Slev2 and 28Sdes2 (Verovnik *et al.* 2005; Zakšek *et al.* 2007) and with primers Aa_L28S_21, Aa_H28S_1078 (Bayha *et al.* 2010), ITS 1 and ITS 2 regions were amplified with universal primer pair described by White *et al*. (1990), the COI gene fragment was amplified with universal invertebrate primers LCO1490 and HCO2198 (Folmer *et al.* 1994) and 16S rRNA and 12S rRNA with universal primers (Simon *et al.* 1991; Kocher *et al.* 1989). The PCR mixture was made of 30 ng to 50 ng of template DNA, 1.25 U of Top Taq Polymerase (Qiagen, Cat. No. 200203), 1.5 mM $MgCl_2$, 0.5 µM primers, and 0.2 mM dNTPs. The amplification conditions were as follows: 3 min denaturation at 95°C followed by 35 cycles of 1 min at 95°C, 1 min at 48°C, 90 s at 72°C and terminated with a 5 min extension at 72°C. PCR products were sequenced by a commercial service (Macrogen, Amsterdam, Netherland and IGA Udine, Italy) and the same primer pairs were used for cycle sequencing as for previous PCR. Samples were sequenced in the forward and reverse direction to assure the accuracy of each polymorphic site. GenBank accession numbers of retrieved sequences, together with sequences used as an outgroup, are listed in Table 2.

Sequence alignment

Contigs were assembled and edited using ChromasPro 1.7.6 (Technelysium Pty Ltd, Queensland, Australia). The homologous sequences for comparisons were searched using the BLAST algorithm in GenBank. COI sequences were verified with translation into amino acid sequences using Coelenterate mitochondrial code. The length of COI was 655 bp and alignment was gapless, while the length of 28S rRNA was 671 bp, the length of ITS1/ITS2 regions were 300/346 bp, 16S rRNA was 639 bp, and 12S alignment was 410 bp. *Pelagia benovici* sequences of 28S rRNA from a previous study (Piraino *et al.* 2014), as well as sequences of 28S rRNA from archived *Pelagia noctiluca* samples, were included into the analysis (see Table 2). Alignments were done with a separated dataset for each amplified gene and with concatenated sequences together with sequences of outgroup species (see Table 2 for details) using MAFFT 7 (Katoh and Standley

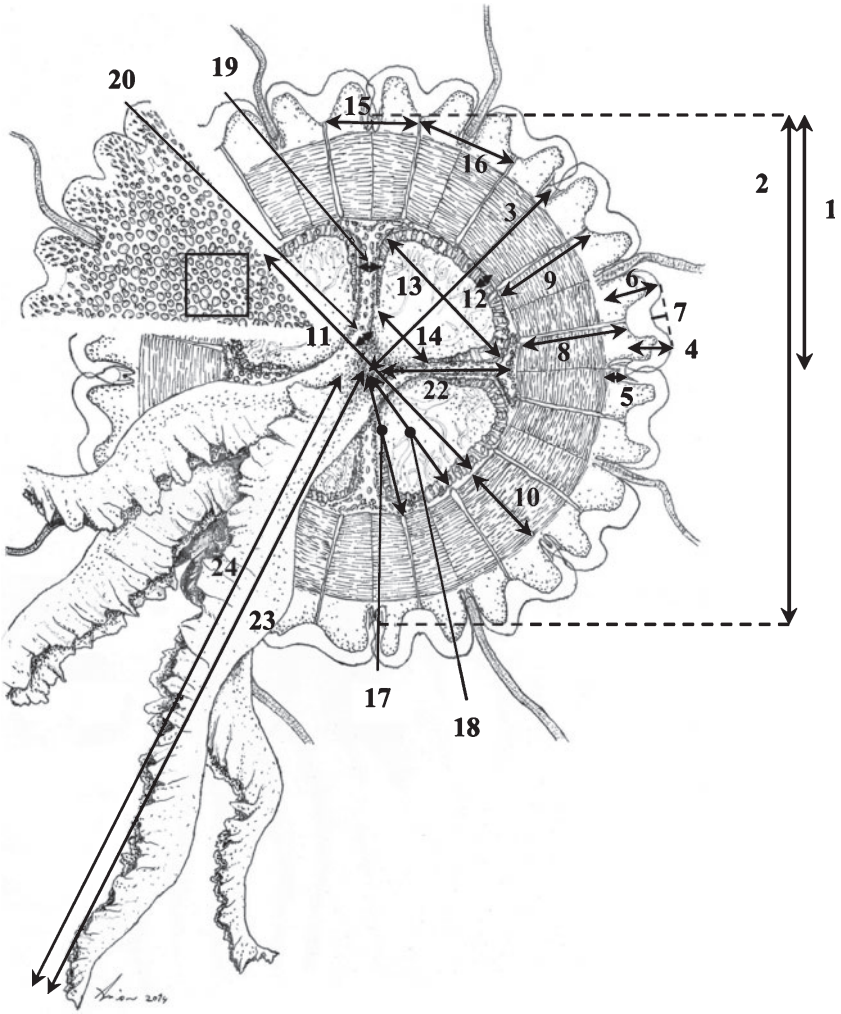

Fig. 3. Drawing of *Mawia benovici*, intentionally performed as similar to the analogous drawing of *Pelagia noctiluca* made by Russell (1970; p. 74, fig. 38), subumbrellar view of adult to show the morphological features considered (in mm). Inset (top left), exumbrellar perspective: (1) perradial radius; (2) bell diameter (perradial, between opposite rhopalia); (3) interradial radius; (4) rhopaliar lappet length; (5) rhopaliar sensory pit depth; (6) tentacular lappet length; (7) marginal lappet cleft; (8) perradial septum length; (9) interradial septum length; (10) coronal muscle width; (11) gonad width (at perradius); (12) largest length between opposite gonads (interradial); (13) largest amplitude of the gonadic arc (distal); (14) smallest amplitude of the gonadic arc (proximal); (15) gastric pouch largest width (perradial, distal); (16) gastric pouch largest width (interradial, distal); (17) length between umbrella centre and origin of perradial septum; (18) length between umbrella centre and origin of interradial septum; (19) basal pillar width (at half of its length); (20) basal pillar, mesogleal thickness at the manubrium emergence; (21) basal pillar, thickness at half of its length (*); (22) basal pillar, length; (23) manubrium plus oral arms total length; (24) manubrium length (*); (25) oral arm length; (26) manubrium mesogleal layer, thickness (*); (27) umbrella mesogleal layer, thickness (*); (28) nr of nematocyst warts per cm^2 (square in the inset – top left); Features marked with (*) are not plotted in the drawing. The feature (24) cannot be measured directly; was obtained by subtracting from the total measure (23) the length of the oral arms (25).

2013). The following default settings were used concerning each set of sequences: scoring matrix: 1PAM/κ = 2 for 28S, 16S and 12S rRNA, while for COI was used 200PAM/κ = 2, gap opening penalty 1.53 (1.0–3.0), offset value 0.00 (0.0–1.0). The scoring matrix was based on the Kimura-2 parameter substitutions model. The combined alignment of COI-16S-12S-28S-ITS1-ITS2 (length 3021 bp) was made from sequences of *Pelagia benovici* (12 specimens), *Pelagia noctiluca* (7 specimens), *Sanderia malayensis* (1 specimen), *Chrysaora hysoscella* (2 specimens) and the outgroup species *Cyanea capillata* (Linnaeus, 1758) (1 specimen). Concatenated sequences were made of sequences amplified from the same individuals of *P. benovici* (collected

Table 2. List of sequences from *Mawia benovici*, *Pelagia noctiluca*, *Sanderia malayensis*, *Chrysaora* spp., and *Cyanea capillata* (outgroup) used for phylogenetic analysis according to genetic marker

Family	Species	Isolate	Genetic marker GenBank Accession number (haplotype name)					
			COI	28S	16S	12S	ITS1	ITS2
Pelagiidae	*Mawia benovici*	2	KM015222(1-COI)	KM217190(1-28S)	KM217205(1-16S)	KM036489(1-12S)	KM217234(1-ITS1)	KM036431(1-ITS2)
	Mawia benovici	9	KM015228(1-COI)	KJ697773(1-28S)	KJ697779(1-16S)	KM036490(1-12S)	KM217235(1-ITS1)	KM036435(1-ITS2)
	Mawia benovici	11	KM015230(1-COI)	KJ697774(2-28S)	KJ697780(1-16S)	KM036491(1-12S)	KM036464(1-ITS1)	KM036436(1-ITS2)
	Mawia benovici	14	KM015233(1-COI)	KM217191(2-28S)	KM217206(3-16S)	KM217222(1-12S)	KM036465(1-ITS1)	KM036438(1-ITS2)
	Mawia benovici	16	KM015234(1-COI)	KM217192(1-28S)	KJ697781(1-16S)	KM036492(1-12S)	KM036466(1-ITS1)	KM036439(1-ITS2)
	Mawia benovici	17	KM015235(1-COI)	KM217193(2-28S)	KJ697782(1-16S)	KM036493(1-12S)	KM036467(1-ITS1)	KM036440(1-ITS2)
	Mawia benovici	25	KM015240(1-COI)	KM217195(2-28S)	KM217207(4-16S)	KM217223(1-12S)	KM036470(1-ITS1)	KM036444(1-ITS2)
	Mawia benovici	30	KM015243(2-COI)	KM217196(2-28S)	KM217209(5-16S)	KM217224(1-12S)	KM036474(1-ITS1)	KM036449(1-ITS2)
	Mawia benovici	36	KM015246(1-COI)	KM217198(1-28S)	KJ697784(1-16S)	KM036496(1-12S)	KM036479(1-ITS1)	KM036454(1-ITS2)
	Mawia benovici	39	KM015249(1-COI)	KM217199(3-28S)	KJ697785(1-16S)	KM036497(1-12S)	KM217237(2-ITS1)	KM036457(2-ITS2)
	Mawia benovici	44	KM015252(1-COI)	KM217200(1-28S)	KJ697786(1-16S)	KM036498(1-12S)	KM036483(1-ITS1)	KM036459(1-ITS2)
	Mawia benovici	50	KM015257(4-COI)	KM217202(2-28S)	KM217210(6-16S)	KM217225(1-12S)	KM036488(1-ITS1)	KM036460(1-ITS2)
	Pelagia noctiluca[A]	*NSAM00001P*		KJ573407(4-28S)				
	Pelagia noctiluca[A]	NSAM00001N		KJ573405(5-28S)				
	Pelagia benovici[A]	NSAM00036B		KJ573396(6-28S)				
	Pelagia noctiluca	*PN1H*	KM651785	KM217177	KM217211	KM217226	KM217239	KM217248
	Pelagia noctiluca	*PN2H*	KM651786	KM217183	KM217212	KM217227	KM217240	KM217249
	Pelagia noctiluca	*PN9H*	KM651787	KM217185	KM217231	KM217228	KM217241	KM217250
	Pelagia noctiluca	*PN11M*	KM651792	KM217179	KM217217	KM217229	KM217243	KM217251
	Pelagia noctiluca	*PN12M*	KM651794	KM217180	KM217218	KM217230	KM217244	KM217252
	Pelagia noctiluca	*PN14M*	KM651793	KM217186	KM217219	KM217231	KM217245	KM217253
	Pelagia noctiluca	*PN17M*	KM651795	KM217182	KM217220	KM217232	KM217246	KM217254
	Pelagia noctiluca	*PN0803*		KM873332				
	Pelagia noctiluca	*PN1108*		KM873333				
	Pelagia noctiluca	*PN1307*		KJ697778				
	Pelagia noctiluca	M0D14612Z		HM194865				
	Pelagia benovici[A]	*NSAM000036G*		KJ573401				
	Pelagia benovici[A]	*NSAM000036H*		KJ573402				
	Pelagia benovici[A]	*NSAM00036F*		KJ573400				
	Pelagia benovici[A]	*NSAM000036I*		KJ573403				
	Sanderia malayensis		KR054756	HM194861	JX393267			
	Chrysaora hysoscella	*1*	KM651796	KM651814	KM651801	KM873331	KM651836	KM651820
	Chrysaora hysoscella	*2*		KM651815	KM651802		KM651837	KM651821
	Chrysaora hysoscella	*4*	KM651797	KM651817	KM651804	KM873331	KM651839	KM651823
	Chrysaora hysoscella	*5*		KM651818	KM651805		KM651840	KM651824
	Chrysaora hysoscella	*6*		KM651819	KM651806	KM873331	KM651841	KM651825
	Chrysaora sp.	*EK-2011*	JN700941	AY920779	JN700941	JN700941	DQ083525	No data
	Chrysaora lactea			HM194863				
Cyaneidae	*Cyanea capillata*		JN700937	HM194873	JN700937	JN700937	No data	No data

[A]Sequences from Piraino *et al*. (2014) and reclassified according to diagnostic indels in 28SrDNA (see Results section).

in this study), *P. noctiluca*, and *C. hysoscella* produced during this study, while in other species concatenated sequences were made of available sequences regarding the genes (see Table 2 for details). The dataset of 28S rRNA consisted of sequences of *P. benovici*, *P. noctiluca*, *C. hysoscella*, *C. lactea*, *Chrysaora* sp., *S. malayensis* and *C. capillata* as the outgroup.

Phylogenetic analysis

Each dataset for phylogenetic analysis was composed of unique haplotypes from nuclear and mitochondrial genes (28S, ITS1/ITS2, COI, 16S, 12S) used in alignments as described in the previous section. A phylogeny inference was done separately on each dataset and on combined alignment, which included species from all the valid genera of Pelagiidae (*Pelagia*, *Chrysaora* and *Sanderia*). A test of substitution saturation was performed for COI haplotypes as described by Xia *et al.* (2003) using the software Dambe v5.3.108, and no saturation with substitutions was found. The best models of substitution under the Akaike Information Criterion (AIC) were: GTR+I+G ($\alpha = 1.008$) for COI, GTR+G ($\alpha = 0.459$) for 28S, GTR+G ($\alpha = 0.335$) for 12S, GTR+I+G (with $\alpha = 0.813$) for 16S, GTR+I+G ($\alpha = 1.134$) for ITS1, and SYM+G ($\alpha = 0.437$) for ITS2. jModeltest v2.1.1 (Darriba *et al.* 2012) was used for calculations. Phylogenetic analyses were run with MrBayes v3.2.1 (Ronquist and Huelsenbeck 2003) with four chains for 2×10^6 generations, sampled every 1000 generations, discharging the first 25% of samples as burn in and run until stationarity was reached (Figs 11, 12). For each gene, we used models suggested by AIC or the most similar one available in MrBayes. Stationarity was checked against plotted values, and MCMC was used to estimate posterior probability distribution using Tracer v1.6.0 (Rambaut *et al.* 2014). Trees were visualised in FigTree v1.4.2 (Rambaut 2006). Furthermore, a maximum likelihood (ML) tree was calculated using the same set of concatenated genes in RaxML v8.2.8 (Supplementary Material 5; Stamatakis 2014) and setting *C. capillata* as the outgroup. RaxML was run online on the CIPRES Science Gateway portal v3.3 (Miller *et al.* 2010). RAxML Workflow interface was followed for the ML using Maximum Likelihood/Thorough Bootstrap approach and GTRGAMMA model and autoMRE criterion to assess the saturating number of bootstrap resampling (504 bootstraps). The evolutionary distances between haplotypes at each locus were calculated among and within pelagiid species using the Kimura-2 parameter model (K2P) in MEGA v6.0 (Tamura *et al.* 2013).

Cladistic analysis

Cladistic analyses were based on a set of morphological characters we considered as genus-specific within the family Pelagiidae. We used a genus of the family Cyaneidae (*Cyanea* Péron & Lesueur, 1810) as an outgroup, and within the family Pelagiidae, all valid species were considered (*Sanderia* Goette, 1886; with *S. malayensis* and *S. pampinosus* Gershwin & Zeidler, 2008; *Chrysaora* Péron & Lesueur, 1810, with *C. achlyos* Martin, Gershwin, Burnett, Cargo & Bloom, 1997, *C. chinensis* Vanhöffen, 1888, *C. colorata*, *C. fulgida* (Reynaud, 1830), *C. fuscescens*, *C. hysoscella*, *C. kynthia* Gershwin & Zeidler, 2008, *C. lactea*, *C. melanaster* Brandt, 1835, *C. pacifica* (Goette, 1886), *C. pentastoma* Péron & Lesueur, 1810, *C. plocamia* (Lesson, 1830), *C. quinquecirrha* (Desor, 1848), *C. wurlerra* Gershwin & Zeidler, 2008; *Pelagia* Péron & Lesueur, 1810, with *P. noctiluca* and *P. benovici*. We have not considered *species inquirendae*, as *C. caliparea* (Reynaud, 1830), or *species dubiae*, as *P. cyanella* Péron & Lesueur, 1810, *P. flaveola* Eschscholtz, 1829, and *P. panopyra* Péron & Lesueur, 1810.

The data matrix contains 32 characters (Table 3) for each genus, coded as binary when possible, or multistate, and considered as unordered. Characters that were not available are coded as –, unknown characters are marked as ?. Characters of the *Cyanea* genus, some *Chrysaora* species and *S. pampinosus* not directly observed in the present work were taken from literature (Mayer 1910; Russell 1970; Dawson 2005*a*; Gershwin and Zeidler 2008*b*; Morandini and Marques 2010; Holst and Laakmann 2014). The maximum parsimony tree of morphological characters was made by branch-and-bound search using the cladistic option in the software PAST v2.17 (Hammer *et al.* 2001) and 500 bootstrap replicates were used. The gene tree (mtDNA, 28S and ITS) was analysed together with the 32 genus-level morphological characters (see Table 3)

Table 3. Data matrix of 32 characters of pelagiid genera and one cyaneid (outgroup)

For characters' description see 'Results'. – = data not available, ? = unknown

Morphological character	Pelagiid genera				Outgroup
	Sanderia	*Mawia*, gen. nov.	*Chrysaora*	*Pelagia*	*Cyanea*
1	0	0	0	0	1
2	1	0	0	1	2
3	1	0	0	0	0
4	0	1	1	0	0
5	0	1	1	0	0
6	0	1	1	0	–
7	1	0	0	1	–
8	0	0	0	0	1
9	1	0	2	0	3
10	0	0	1	0	1
11	0	0	1	0	2
12	1	0	0	0	0
13	0	0	1	3	2
14	1	0	2	0	0
15	1	0	0	0	0
16	3	0	2	0	1
17	0	1	2	1	3
18	0	0	2	0	1
19	1	0	2	0	3
20	0	1	2	3	1
21	0	0	1	0	2
22	0	0	0	0	1
23	1	0	3	2	4
24	1	0	2	2	2
25	1	0	0	0	0
26	1	1	0	0	0
27	2	1	3	1	0
28	2	1	3	4	0
29	0	0	1	0	0
30	0	0	0	1	0
31	0	0	0	1	0
32	0	?	0	1	0

in MrBayes 3.2.1 under the same conditions as concatenated sequences only.

Results

Systematics

According to the examined morphological features and phylogenetic position described in the next section, we conclude that *Pelagia benovici* must be classified into a genus novum.

Genus ***Mawia***, gen. nov.

http://zoobank.org/urn:lsid:zoobank.org:act:7C8A7B22-6D21-4208-B615-BAA86188C200

Type species: *Pelagia benovici* Piraino, Aglieri, Scorrano & Boero, 2014

Type locality: Northern Adriatic: from the Gulf of Venice to the Gulf of Trieste.

Generic diagnostic characters for genus Mawia

A pelagiid with marginal tentacles without mesogleal folds, or adaxial furrow, or thickenings; basal pillars Y-shaped, slight, lateral distal branches short, slightly curved inwards, single arch cross-section, proximal portion thicker, right triangle-shaped from a lateral view; horseshoe-shaped gonads, simple folded ribbon-like, with concavity facing the manubrium, slightly protruding; covered by nematocyst warts; subgenital pouch – wide flat area, leaf clover-shaped, gonad folds slightly protruding in the distal area; exumbrellar sensory pit shallow, ovoidal, longitudinal section as a right triangle, with the minor cathetus (facing outwards) ~1/3 of the larger cathetus, the distal edge emphasised by nematocyst warts, of glass-like transparency.

Etymology

The genus name is derived from the Latin form of the name of *Māwiyya*, a legendary warrior queen who ruled over an Arab confederation in southern Syria in the latter half of the fourth century.

Mawia benovici (Piraino, Aglieri, Scorrano & Boero, 2014), comb. nov.

Material examined

Holotype. Male specimen (adult), collected from the Gulf of Venice (Chioggia), November 2013, with a 46 mm umbrella diameter. Deposited in the Collection of the Museum of Adriatic Zoology Giuseppe Olivi (Palazzo Grassi, Chioggia, Padova University). Accession number: CN54CH (Piraino *et al.* 2014).

Paratype 1. Female specimen (adult), Gulf of Venice (Chioggia), November 2013, 50 mm diameter of umbrella. Deposited in the Collection of the Museum of Adriatic Zoology Giuseppe Olivi (Palazzo Grassi, Chioggia, Padova University). Accession number: CN55CH (Piraino *et al.* 2014).

Other material examined. 10 specimens. Gulf of Venice (Chioggia), November 2013, 32–45 mm (range of bell diameter). Deposited in the Collection of Marine Invertebrates at the Laboratory of Zoology and Marine Biology of the University of Salento (Lecce). Accession numbers: UNIS_SCY_001–10.

Remarks

The reported morphological descriptions are based on the following additional material: six specimens, all males, and deposited in the collection of the Trieste Natural History Museum, Via dei Tominz 4, Trieste. One was collected on 6 December 2013 outside the harbor of Santa Croce, with a 57 mm umbrella diameter (accession number: Im/CNI 060–060); three specimens collected near Piran on 4 December 2013, with umbrellar diameters of 68, 69, and 67 mm, respectively (accession number: Im/CNI 060–061 to –063); and two preserved specimens collected in 2004 and analysed for the first time during this study, one collected on 28 June outside the harbor of Santa Croce with an umbrellar diameter of 70.5 mm, and one on 11 November in the Gulf of Trieste near Piran with an umbrellar diameter of 63 mm (accession number: Im/CNI 060–064 and –065).

Species morphological description

Morphological characteristics of the species are presented in Figs 2–4 and 9–10 while Figs 5, 6, 7 and 8 show a comparison of specific characteristics with some other pelagiid species. The detailed new description is below:

The umbrella diameter of specimens ranges from 3 to 7 cm and is hemispherical to somewhat flattened, with a thick, but rather soft mesogleal layer, is inconsistent, has eight adradial marginal tentacles, and eight per- and interradial rhopalia. Medusa with 16 marginal lappets, rounded lateral portions, and a slight cleft (its depth is variable even in a single specimen) between them, with a mean depth of 1.7 mm ($n = 6$, Fig. 4*b*). Their lateral portion is thicker, due to the presence of two gastric pouch extensions, one tentacular and one rhopaliar, which terminate in an irregular rounded end. The intermediate areas and the margins are very thin and transparent (Figs 3, 4*b*, *d*). Preliminary observations about its pulsation rate indicate a pulsation rate of 60 pulsations/min at a temperature of 18°C in laboratory conditions (Feb. 21st, 2014, Supplementary Material 4), and ~20 pulsations/min at a temperature of 11.5°C in a natural environment. In field observations, *Mawia benovici*, if disturbed, let itself sink without pulsating or turning downwards.

Hollow tentacles originate from an ellipsoidal, slightly downward sloping area, the exumbrellar margin of the tentacular niche is fused over the proximal portion of the tentacle (Fig. 5*b*). The transverse section of a tentacle shows a regular outer epidermal layer, an underlying homogeneous layer of mesoglea and an innermost gastrodermic layer, which delimits the tentacular canal of the gastro-vascular apparatus. There is no evidence of ectodermal, muscular folds into the mesogleal layer (Fig. 5*d*), nor subumbrellar longitudinal furrows or thickenings. Relaxed tentacles can exceed a length of more than three times the bell diameter.

The *rhopalia* (Fig. 4*e*, *f*) are housed in rhopaliar niches. In living or freshly fixed specimens, the statocyst shows an ellipsoid shape, dark brown to black in colour. The pits that are present laterally to the base of the rhopalium exhibit horizontal brownish stripes that tend to fade quickly in fixed specimens (Fig. 4*e*). The brownish stripes disappear a couple of weeks after fixation.

The *exumbrellar sensory pits* are placed over the rhopaliar base, are ovoidal in aspect with the apex pointing outwards, slightly depressed, with the deepest point in correspondence of the distal margin; the longitudinal section corresponds approximately to a right triangle, with the minor cathetus

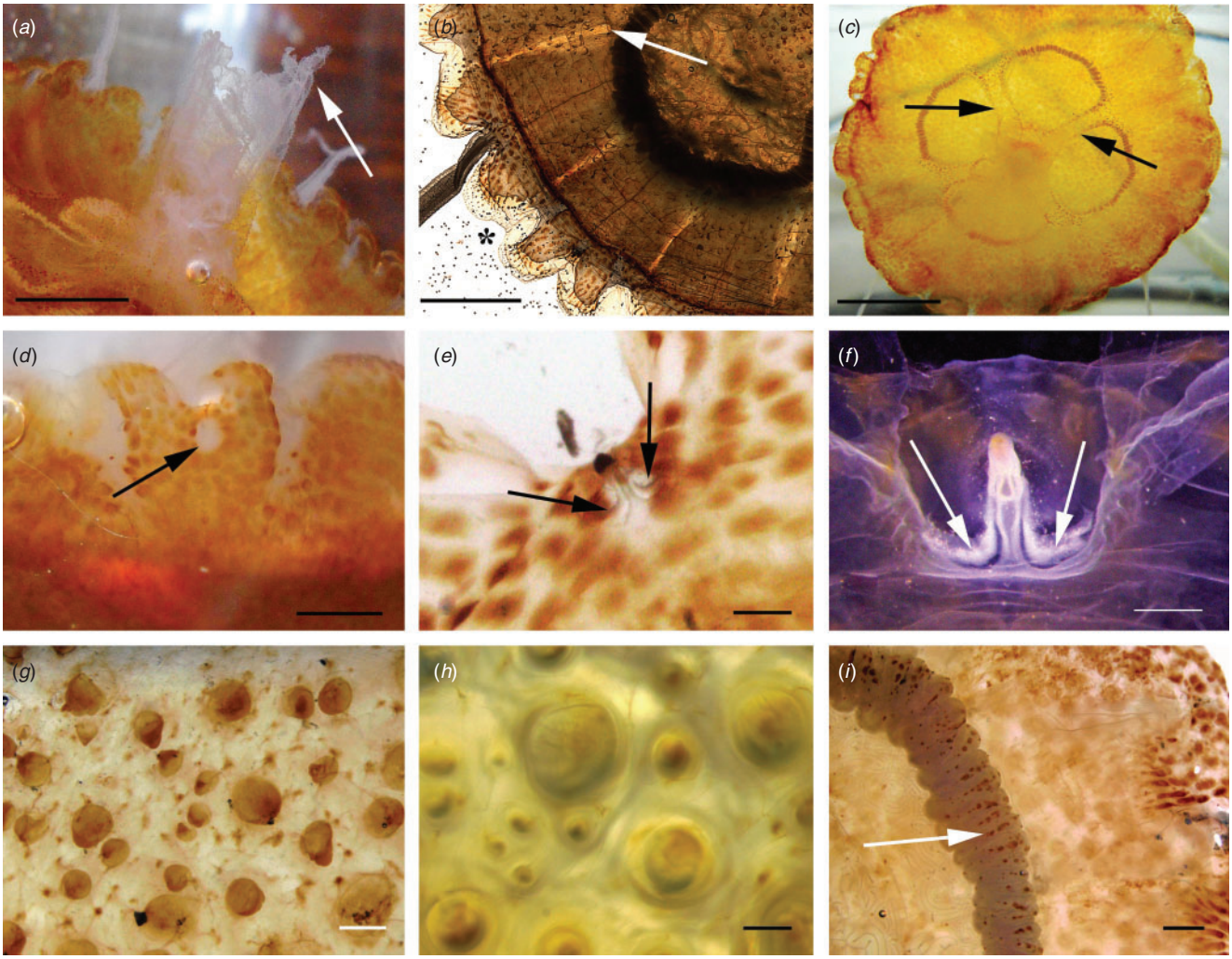

Fig. 4. *Mawia benovici*: (*a*) living specimen showing a short manubrium and small oral arms (arrow); (*b*) preserved specimen, exumbrellar view of the straight radial septa, with rounded proximal edge (arrow), and marginal lappets (scale bar = 1 cm). Asterisk indicates the cleft present in the middle of the marginal lappets; (*c*) preserved specimen, subumbrellar view showing the pattern of basal pillars (arrows; scale bar = 1 cm); (*d*) living specimen showing the exumbrellar glass-like area, which contains the sensory pit (arrow; scale bar = 1 cm); (*e*) living specimen, exumbrellar view of a rhopalium. Arrows indicate the dark stripe present in the lateral niches (scale bar = 2 mm); (*f*) dark field micrograph of a rhopalium as in (*f*); (*g*) living specimen, exumbrellar magnification showing the weakly protruding papillar warts, with darker tip (scale bar = 1 mm); (*h*) higher magnification of some exumbrellar warts (scale bar = 0.5 mm); (*i*) living specimen, subumbrellar view of one folded ribbon-like gonad, covered with nematocyst warts (arrow; scale bar = 1 mm).

distal (Fig. 7*d*), and with a mean LM ratio of 0.279 and a mean AS ratio of 0.239 ($n = 4$). The distal margin of the sensory pit is very distinctive, as it is covered by a row of nematocyst warts (Fig. 7*b*). This area in living specimens is of a glass-like transparency, obvious even to the naked eye (Fig. 4*d*).

The *exumbrella* is smooth when touched, even if the exumbrellar surface is uniformly covered with densely packed nematocyst warts, whose shape vary from circular to elliptical, or more narrow and elongated at the level of marginal lappets (Figs 2*c*, 3, 4*g*, *h*, *i*). Warts are only present over the two gastric pouches (tentacular and rhopaliar) extensions on both sides of each lappet (Fig. 4*b*, *d*). The warts are not thick. The larger warts with pigmented apex can be seen in the central exumbrellar area of living specimens (Fig. 4*g*, *h*), with a weak, fluffy consistency. *M. benovici* exhibits a mean number of nematocyst warts/cm^2 of 128 (Supplementary Material 2).

The *subumbrellar surface* just before the rhopaliar and tentacular pits shows a well developed coronal muscle (Figs 3, 4*b*), which seem divided (it's just an optical effect) by the presence of 16 straight radial septa. Each division has a thin, radial irregular line just in the middle, in correspondence with every rhopalium and tentacle (Figs 3, 4*b*). Along the perradia, there are four long, narrow bases of the manubrium (*oral* or *basal pillars*). Each of them starts peripherally with a Y- or T-shaped, slightly thickened structure, with lateral distal branches short, slightly curved with concavity facing inwards, and the main radial branch narrow and semicircular or arc-shaped in the cross-section, with parallel lateral edges. Near the emergence of the

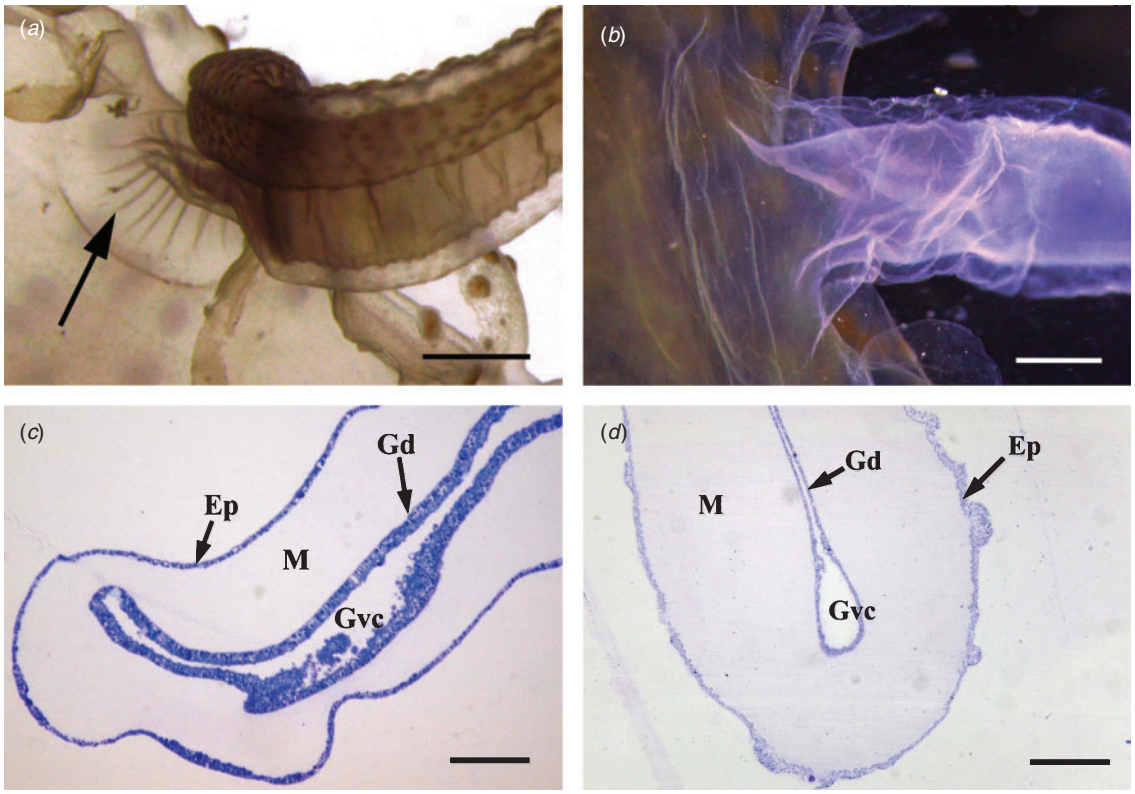

Fig. 5. Tentacle characteristics: left *Sanderia malayensis* (*a*, *c*), right *Mawia benovici* (*b*, *d*). (*a*) *Sanderia malayensis*, light micrograph of the area of emergence of one tentacle, subumbrellar view (scale bar = 1 mm), arrow indicates one of the thin, subumbrellar epidermic furrows; (*b*) *Mawia benovici*, dark field micrograph of the area of emergence of one tentacle, subumbrellar view (scale bar = 1 mm); (*c*) *Sanderia malayensis*, tentacular semi-thin transverse section, adaxial area (scale bar = 150 µm); (*d*), *Mawia benovici*, tentacular semi-thin transverse section, adaxial area (scale bar = 150 µm). Ep, epidermis; Gd, gastrodermis; Gvc, gastrovascular canal; M, mesoglea.

manubrium, each pillar increases in thickness, thus forming a sort of right triangle – if observed laterally – downwardly projecting which continues in the manubrium (Figs 3, 4*c*, 9*a*).

The *stomach* is simple, without interradial septa, with four interradial, subumbrellar ribbon-like folded gonads, with distal free edges (Figs 4*b*, *c*, 9*a*).

The four *gonads* are horseshoe-shaped. There is not a real subgenital pouch or ostium, but rather a thin transparent surface, leaf clover-shaped, bound by the basal pillars laterally, by the gonads distally, and by the manubrium proximally. The layer under the gonads tends to follow their folded ribbon-like shape, protruding a little downwards, but the topography of the gonad is stable, there are not foldings of the IInd or IIIrd order, highly protruding downward as in *Pelagia* or *Chrysaora*. Some hundreds of *gastric cirri* (or filaments) emerge from four subumbrellar areas adjacent to the gonads. Their length is variable, with some of them longer than 2 cm in length, with tips that can protrude into the basal opening of the manubrium (Figs 2*d*, 3, 4*b*, *c*, *i*, 9*a*).

The *gastrovascular sinus* is divided into 16 pouches (eight rhopaliar and eight tentacular, all alike) by 16 straight gastric septa (Figs 4*b*, 9*a*). They are thicker proximally, with a rounded edge, just over the coronal muscle area, with a distal termination in the cleft of marginal lappets equidistant from tentacles and rhopalia. They give origin distally to the small tentacular and rhopaliar lateral pouches inside the marginal lappets. The shape of the lateral pouches is irregularly rounded (Fig. 4*b*). The tentacular pouches continue into the tentacular canals, and the rhopaliar pouches into the rhopaliar canals. A ring canal is absent.

The *manubrium* arises centrally from the perradial basal pillars, and distally is divided into four oral arms, sometimes very long, the margins of which are thin and highly frilled. The oral arms are U-shaped in cross-section, with the thicker section at the base. The length of the whole manubrium can reach up to three times or more than the bell diameter, whilst the oral tube can be very short, and very difficult to detect (Figs 2*c*, 3, 9*d*, *e*). Some specimens exhibit, on the contrary, short oral arms with a long oral tube up to almost half of the total length (Fig. 4*a*). There is a mesogleal layer inside, thicker in correspondence to the outer portion, but the whole manubrium consistency is extremely weak, or flaccid, and in samples placed on a Petri dish without liquid, it collapses completely (Fig. 9*d*).

The *subumbrellar nematocyst warts* have the same shape as the exumbrellar warts, sometimes a little more elongated, and are present on the basal pillars and under the gonad foldings – but not on the subgenital area (Fig. 4*i*). The oral arms and

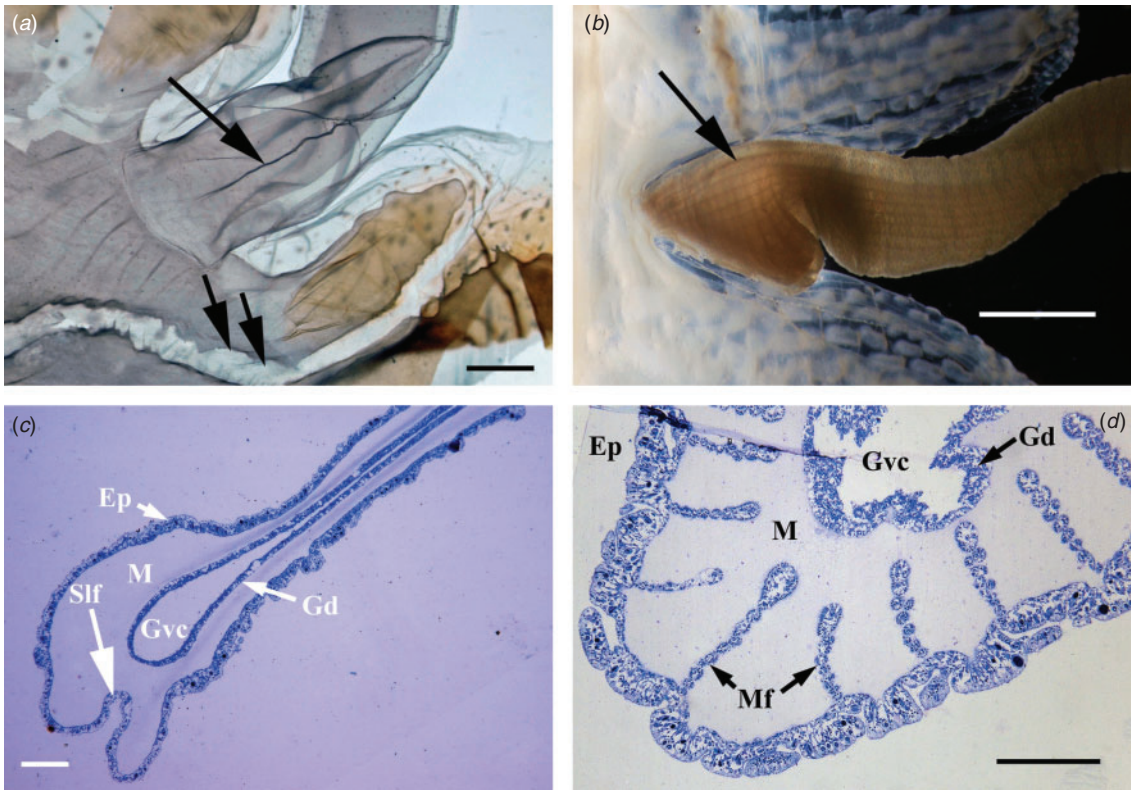

Fig. 6. Tentacle characteristics: left *Chrysaora hysoscella* (*a*, *c*), right *Pelagia noctiluca* (*b*, *d*). (*a*) *Chrysaora hysoscella*, dark field micrograph of the area of emergence of one tentacle, adjacent to a rhopalium (bottom), subumbrellar view. The arrow indicates the adaxial longitudinal furrow; double arrows indicate the curved, S-shaped distal portion of a radial septum (scale bar = 1 mm); (*b*) *Pelagia noctiluca*, dark field micrograph of the area of emergence of one tentacle. The arrow indicates the presence of the epidermal longitudinal muscular folds (scale bar = 1 mm); (*c*) *Chrysaora hysoscella*, tentacular semi-thin transverse section, adaxial area (scale bar = 150 µm); (*d*) *Pelagia noctiluca*, tentacular semi-thin transverse section, adaxial area (scale bar = 150 µm). Ep, epidermis; Gd, gastrodermis; Gvc, gastrovascular canal; M, mesoglea; Mf, epidermal muscular folds; Slf, subumbrellar (or adaxial) longitudinal furrow.

the manubrium have no warts, but are covered by many small protrusions with an apical cluster of nematocysts (detectable only under a stereomicroscope, Fig. 9*d*, *e*).

Gonad histology: the specimens collected and measured in 2013 and in 2014 were males and their testes were analysed. All specimens observed exhibit well developed spermatozoa, at least within some follicles (Fig. 9*c*), regardless of size (from 3 to 7 cm in diameter). From the subumbrellar layer, just distal to the gastric cirri area, a thin fold protrudes, which leans against the floor of the stomach, thus limiting a tiny genital sinus that communicates with the main stomach cavity outwardly (Fig. 9*b*, *c*). At present, the single specimen labelled as female is the Paratype I, of 5 cm in diameter, but no oocytes in advanced stages of maturation were observed during our reexamination under a steromicroscope, which may indicate an immature ovary.

Cnidome: the majority of nematocyst observations was based on undischarged capsules, as the nematocysts have not responded to the usual ion-induced discharging agents, like NaSCN, NaI etc. (Avian *et al*. 1991*a*, 1995), and only two discharged nematocyst types were observed under the SEM. However, even though their exact classification is not possible without observation of the discharged tubules, the following nematocyst types can be provisionally assigned: heterotrichous microbasic eurytele (Fig. 10*a*, *d*); O-holotrichous isorhiza (Fig. 10*a*, *b*, *c*); A-holotrichous isorhiza-or heterotrichous isorhiza, depending on the spine morphology (Fig. 10*a*, *e*); a smaller capsule that could be assigned to an a-holotrichous isorhiza (or heterotrichous, as the previous) or atrichous isorhiza (Fig. 10*a*, *f*); a big ovoid capsule with a large operculum, but with an unclear undischarged tubule morphology (at present it is not possible to state the presence – or not – of a shaft, Fig. 10*g*); and finally a nematocyst with a very elongated, ellipsoid capsule, containing a shaft whose length is almost equal to the larger diameter of the capsule (a p-mastigophore?, Fig. 10*h*). A possible presence of birhopaloid type II, as suggested by Piraino *et al*. (2014), without SEM analyses, cannot be confirmed.

Colouration is mainly determined by the ex- and sub-umbrellar nematocyst warts, which are orange-reddish to purple in colour. Umbrellar mesoglea, tentacles, manubrium, and oral arms are colourless (Figs 2*c*; 4*a*, 9*d*, *e*). All the specimens we observed were males, and testes vary from ivory white to pale sandy (Figs 2*a*; 4*i*). The pale pink to fuchsia gonads of some living specimens photographed in November 2004 (Fig. 2*d*) were never observed in specimens collected in this study. There is also a slight colour variation between the specimens observed in 2004 and 2013: some specimens from

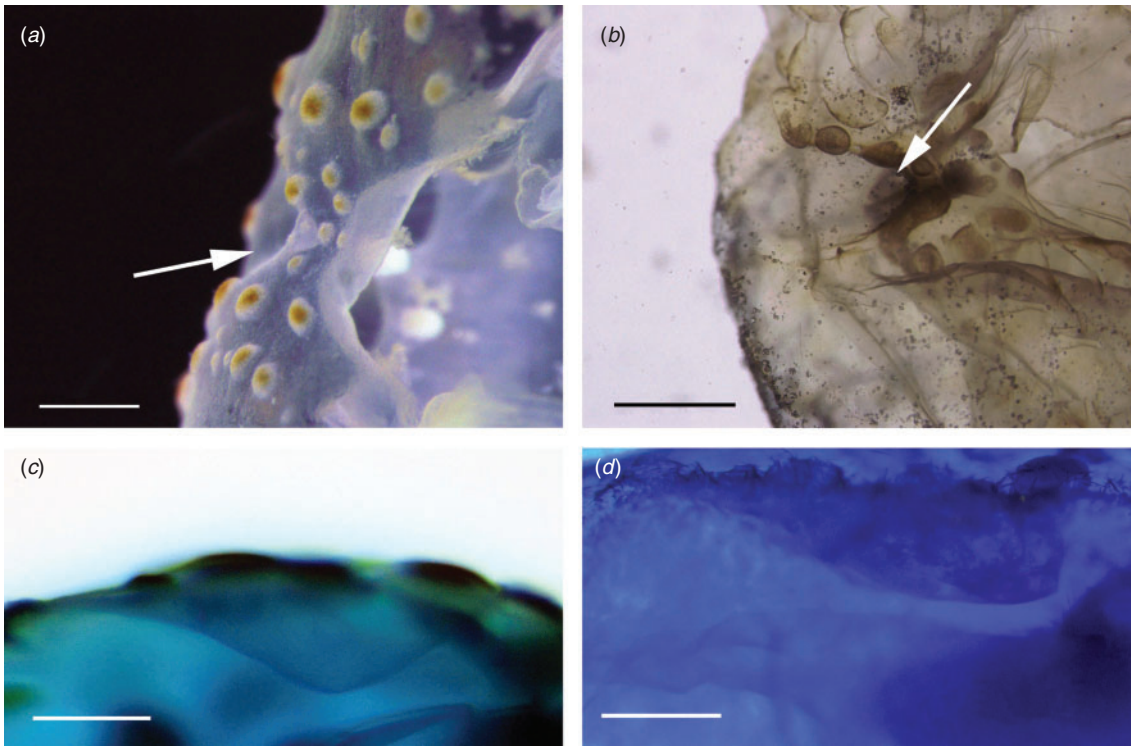

Fig. 7. Exumbrellar sensory pit: left *Sanderia malayensis* (*a*, *c*), right *Mawia benovici* (*b*, *d*). (*a*) *Sanderia malayensis*, exumbrellar sensory pit, distal view. The arrow indicates the concavity of the sensory pit, with the deepest point visible in transparency (scale bar = 1 mm); (*b*) *Mawia benovici*, exumbrellar sensory pit, distal view. The arrow indicates the nematocyst warts on the distal edge of the sensory pit (scale bar = 1 mm); (*c*) *Sanderia malayensis*, sensory pit, lateral view. Distal umbrellar margin on the left (scale bar = 0.5 mm); (*d*), *Mawia benovici*, sensory pit, lateral view. Distal umbrellar margin on the left (scale bar = 0.5 mm).

2004 have reddish and darker colouration of the bell, whilst all the recent (from 2013 to 2014) specimens have a bell with orange-red colouration. The manubrium and oral arms of some 2004 specimens have oral arm frillings with a series of faint pink shades, whilst all the specimens collected-observed from 2013 and 2014 only show colourless oral arms.

Morphological characters at genus level

In order to assess a phylogenetic position of *Mawia* within Pelagiidae, we selected 32 characters, considered at genus level for *Sanderia*, *Mawia*, *Chrysaora* and *Pelagia*, with *Cyanea* as an outgroup (see Table 4).

The results are presented in Table 3. The comparison of characters between *Mawia* and the other pelagiid genera (Table 3) highlights that *Mawia* shares the highest number of similar characters with *Pelagia* (18 characters). In contrast, the highest number of differences in characters was observed with *Sanderia* (19 characters). Moreover, *Mawia* possesses some peculiarities not shared with any other pelagiid genera, like the proximal shape of the radial septa (character 20), the gonad pattern in living specimens (character 23), their degree of folding (character 24), and the shape of basal pillars (character 28). A more detailed description of the morphological features suitable for discriminating Pelagiidae genera is presented in Table 5.

Nematocyst morphology and morphometry were not considered owing to the lack of comparable data in all the studied genera.

Sequences data and haplotypes description

The nuclear gene 28S rRNA and ITS1/ITS2 interspacer regions and parts of three mitochondrial genes COI, 16S rRNA and 12S rRNA were sequenced from *Mawia benovici* specimens collected in the northern Adriatic Sea (Table 1). We amplified the COI from 36 specimens (four unique haplotypes), 28S rRNA from 15 specimens (three unique haplotypes), 16S rRNA was amplified from 15 specimens (six unique haplotypes), 12S rRNA amplified from 16 specimens (one unique haplotype), ITS 1 amplified from 34 specimens (two unique haplotypes), and ITS 2 amplified from 31 specimens (two unique haplotype). A comparison of COI sequences from our 36 specimens and seven COI sequences from a previous study (Piraino *et al.* 2014) revealed five unique COI haplotypes (Table 2). The most abundant haplotype 1-COI was found in 39 sequences from both studies and was represented by the sequence under the accession number KM015222 *Mawia benovici* 2. The other haplotypes were: haplotype 2-COI with accession number KM015243 *Mawia benovici* 30, haplotype 3-COI with accession number KM015254 *Mawia benovici* 46, haplotype 4-COI with accession number KM015257 *Mawia benovici* 50, and haplotype 5-COI represented by *Pelagia*

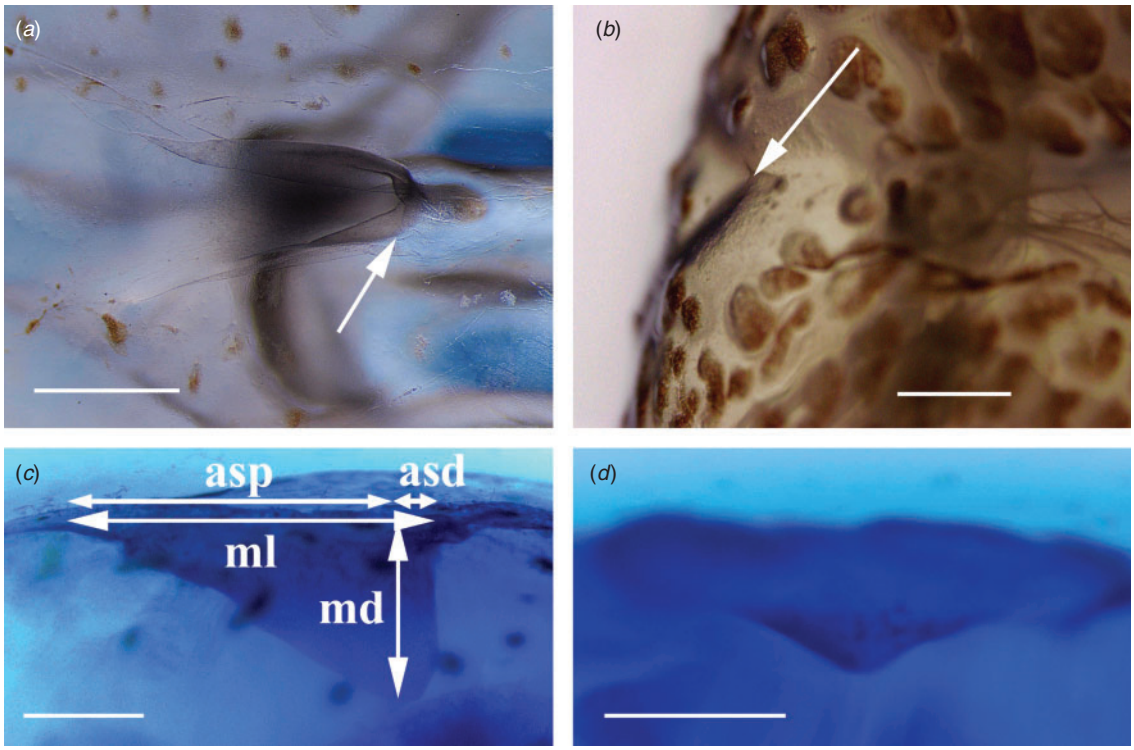

Fig. 8. Exumbrellar sensory pit: left *Chrysaora hysoscella* (*a*, *c*), right *Pelagia noctiluca* (*b*, *d*). (*a*) *Chrysaora hysoscella*, exumbrellar sensory pit, upper view. The arrow indicates the deeper distal edge of the sensory pit (scale bar = 1 mm); (*b*) *Pelagia noctiluca*, exumbrellar sensory pit, distal view. The arrow indicates the pit's embayment (scale bar = 1 mm); (*c*) *Chrysaora hysoscella*, sensory pit, lateral view. Distal umbrellar margin on the left (scale bar = 0.5 mm). asd, distance of the point of maximum depth towards its distal margin; asp, distance of the point of maximum depth towards its proximal margin; md, maximum depth; ml, maximum radial length. (*d*) *Pelagia noctiluca*, sensory pit, lateral view. Distal umbrellar margin on the left (scale bar = 0.5 mm).

benovici NSAM00036B with accession number KJ573409 from Piraino *et al*. (2014).

Part of the 28S rRNA gene was sequenced in 15 specimens, and all specimens were sequenced with primer pair 28Slev2 and 28Sdes2, and some also with primer pair Aa_L28S_21 and Aa_H28S_1078. The first primer pair aligned in D1 and D2 regions (637 bp product), while the second primer pair aligned in D1 and D3 regions, giving a longer product (1080 bp). The longer sequences were aligned and compared with available sequences from *Pelagia benovici* (Piraino *et al.* 2014). The part of sequences from D2 to D3 regions was identical in all examined species (*Mawia benovici*, *Pelagia benovici*, *Pelagia noctiluca*, *Sanderia malayensis*, *Chrysaora hysoscella*), therefore, this part of the sequences was eliminated, and in final alignment only the variable part from D1 to D2 regions of 28S rRNA was used. All the 28S sequences from this study were compared with previously published sequences from *Pelagia benovici* (Piraino *et al.* 2014). Manual inspection of 28S rRNA-aligned sequences revealed differences in four bases which were related with the examined species: *Mawia benovici* and *Pelagia benovici* have GAAG; *Chrysaora hysoscella*, *Chrysaora lactea* (HM194863), and *Chrysaora* sp. (AY920779) have GAGA; *Sanderia malayensis* has GCGG; while in *Pelagia noctiluca* there is a deletion on this site. Taking into account this deletion, as well as the results of the phylogenetic analysis of 28S rRNA haplotypes, it is undoubtedly possible to separate 28S rRNA haplotypes between all examined genera *Pelagia*, *Mawia*, *Sanderia* and *Chrysaora* (Table 2). In contrast to Piraino *et al*. (2014), we did not find any 28S rRNA haplotypes from *Pelagia noctiluca* which would be shared with *Mawia benovici*. In total, six unique 28S rRNA haplotypes were identified (Table 2), and among them, haplotype 1-28S and haplotype 2-28S are the more abundant. The haplotype 1-28S was found in 10 sequences and represented under accession number KM217190 *Mawia benovici* 2, the haplotype 2-28S represented by accession number KJ697774 *Mawia benovici* 11, and haplotype 3-28S represented by sequence with accession number KM217199 *Mawia benovici* 39. Three unique haplotypes were from analysed sequences from the study of Piraino *et al.* (2014), and revealed all the characteristics of *Mawia benovici* haplotypes, which are characterised by the presence of GAAG bases. Our set of data does not confirm hybridisation events among *Mawia benovici* and *Pelagia noctiluca.*

Six haplotypes were found among 16S rRNA sequences. The most numerous was haplotype 1–16S, represented by accession number KM217205 (10 sequences), then 3–16S (two sequences), and the rest of the haplotypes with only one sequence (see Table 2 for details). Only one haplotype was found among 12S rRNA sequences represented by accession number KM036489, while among ITS2 sequences two haplotypes were found (haplotype 1-ITS2 with accession number KM036431, which is most numerous, and haplotype 2-ITS2 with accession

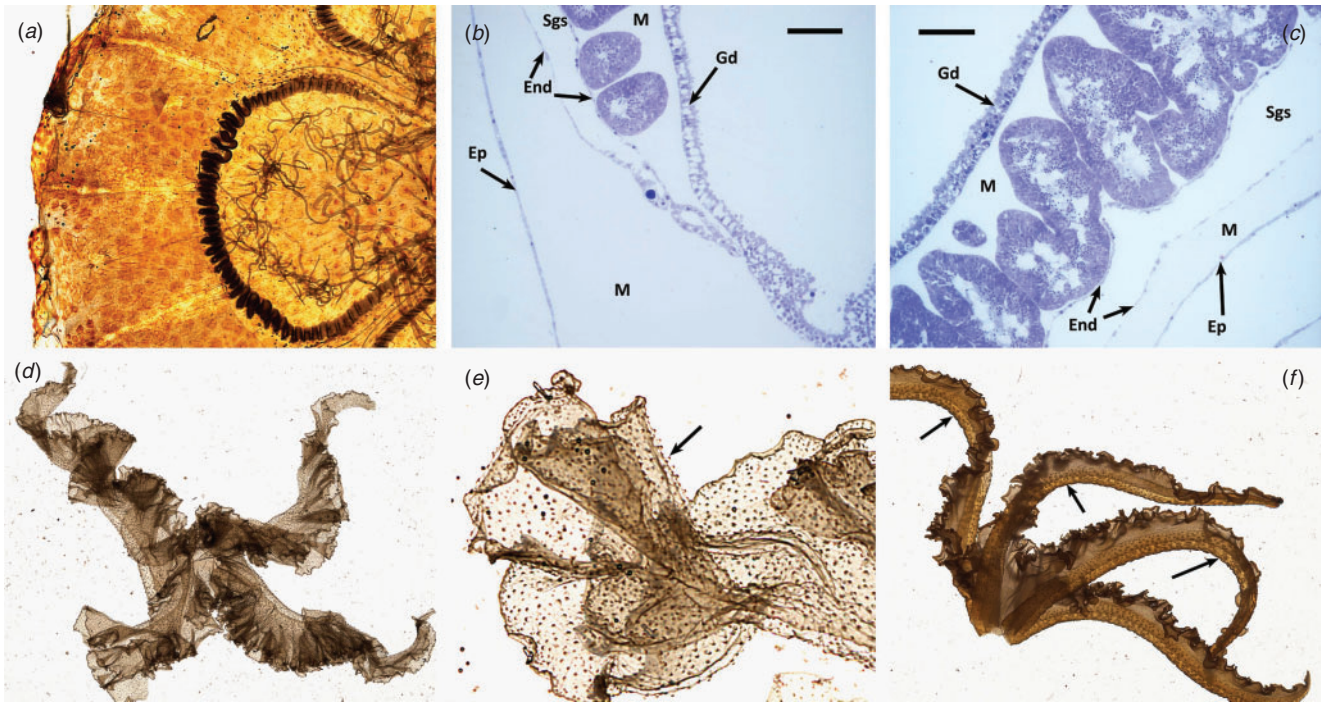

Fig. 9. *Mawia benovici*: (*a*) preserved specimen, exumbrellar view of the overall appearance of one gonad, and the gastric cirri distribution; (*b*) transverse semi-thin section of a testis, in the (proximal) area of protrusion of the gonad ribbon (scale bar = 70 µm). End, genital sinus endoderm; Ep, epidermis; Gd, gastrodermis; M, mesoglea; Sgs, sub-genital sinus. (*c*) as in (*b*), in a more distal area; (*d*), excised manubrium and oral arms, showing the softness of the mesogleal layer, and the absence of large pigmented nematocyst warts; (*e*), magnification of an oral arm frilled margin, showing many very small protrusions (arrow) containing a nematocyst; (*f*), *Pelagia noctiluca*, excised manubrium and oral arms, showing the robustness of the oral arms' medial axis (arrows).

number KM036456). Two haplotypes were found among ITS1 sequences: haplotype 1-ITS1 (accession number KM217234) and haplotype 2-ITS1 (accession number KM217237).

The genetic distances between conspecifics and individuals from different species are used as a threshold in a primary step to delimit species (Pante *et al.* 2015*b*; Meyer and Paulay 2005). Evolutionary distances (Table 6) were calculated for each locus separately using the Kimura-2 parameter model as the best model when distances were low (Nei and Kumar 2000). The closest distance was between *Mawia benovici* and *Sanderia malayensis* at the following loci: COI (0.290 ± 0.33), 16S, and 28S, while for the other loci data were not available for *Sanderia malayensis.* The distance between *Mawia benovici* and *Pelagia noctiluca* at COI locus was 0.399 ± 0.043, while between *Mawia benovici* and *Chrysaora hysoscella* was 0.380 ± 0.040 (Table 6). Haplotype (h) and nucleotide diversity (π) for COI were calculated from the presented dataset (DnaSP 5.10, Librado and Rozas 2009) in order to measure the degree of polymorphism within the population. In *Mawia benovici*, the calculated π was extremely low (below 1% within the examined population) and also COI haplotype diversity ($h = 0.116$).

Phylogenetic analysis

Concatenated sequences were made of a dataset from six genes (COI-16S-12S-28S-ITS1-ITS2) from *Mawia benovici* collected in this study, *Pelagia noctiluca*, *Chrysaora hysoscella*, *Sanderia malayensis*, and *Cyanea capillata* (Fig. 11). The phylogenetic analysis on concatenated sequences (Fig. 11) revealed a highly supported separation (posterior probability 1) between *Pelagia noctiluca* and the rest of analysed species (*Mawia benovici*, *Sanderia malayensis*, and *Chrysaora hysoscella*) as revealed by the Bayesian approach. *Mawia benovici* collected in this study were nested within this group as the closest species to *Sanderia malayensis* (posterior probability 1). Separation between *Sanderia malayensis* and *Chrysaora hysoscella* is highly supported. The ML tree gave the same tree topology with high bootstrap support (97%) at nodes (Supplementary Material 5). Concatenated sequences of *Cyanea capillata* were used as the outgroup in both cases. A comparison of phylogenetic tree and morphological data analysed by Bayesian approach revealed the same results (see Fig. 11). Moreover, the phylogenetic tree of 28S rRNA (Fig. 12) is congruent with the phylogenetic tree made from concatenate sequences: *Mawia benovici* was the closest relative of *Sanderia malayensis* (posterior probability 1). *Chrysaora hysoscella*, *Chrysaora lactea*, and *Chrysaora* sp. formed their own group, separated from group of *Mawia benovici* and *Sanderia malayensis*. Separation of *Pelagia noctiluca* from the rest of the group (*Chrysaora* sp., *Chrysaora hysoscella*, *Sanderia malayensis* and *Mawia benovici*) is also highly supported.

The maximum parsimony tree (MP) obtained by morphological characters based on features at the genus level (Table 3, Fig. 13) produced a highly supported separation of genus *Pelagia* from other genera of Pelagiidae, with genus *Mawia* being the closest to the genus *Chrysaora*, though clearly separated

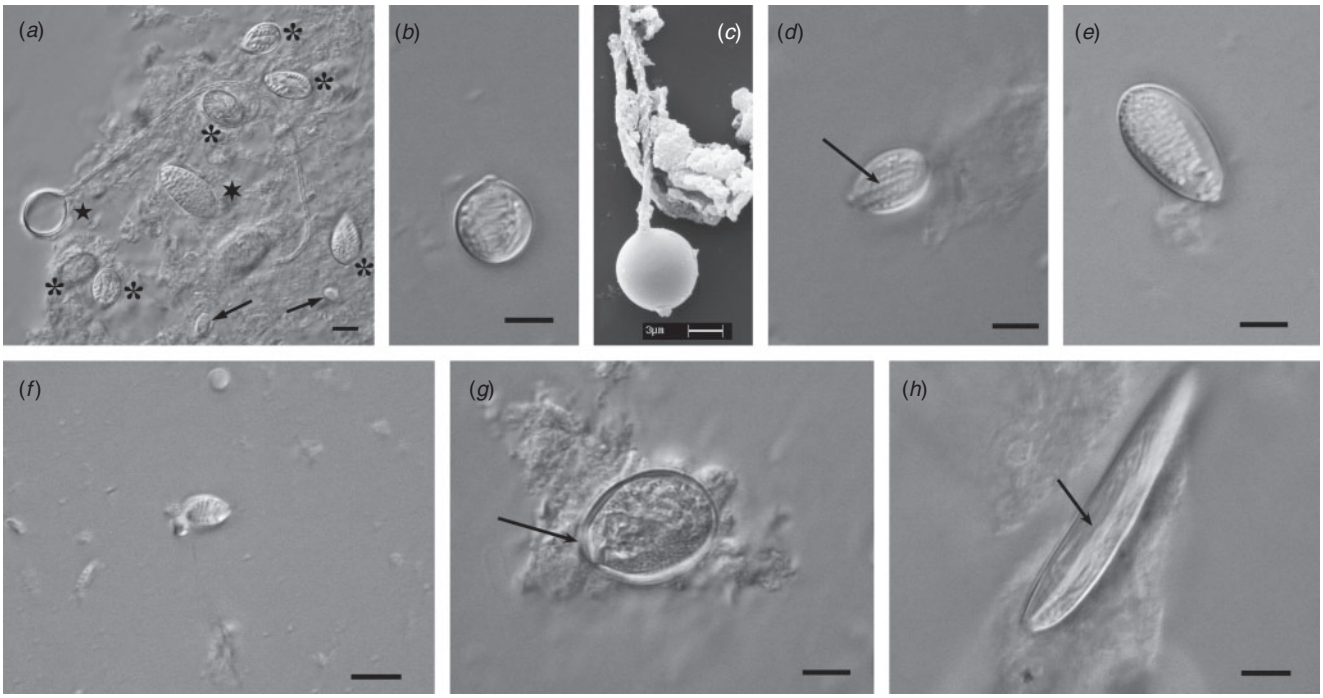

Fig. 10. *Mawia benovici*: (*a*) a light micrograph of a discharged holotrichous O-isorhiza (5 point star), some undischarged microbasic eurytele (asterisks), one undischarged holotrichous A-isorhiza (6 point star) and two undischarged a-isorhiza (arrows; scale bar = 3 µm); (*b*) a light micrograph of an undischarged holotrichous O-isorhiza (scale bar = 3 µm); (*c*) a scanning electron micrograph of a discharged holotrichous O-isorhiza (scale bar = 3 µm); (*d*) a light micrograph of an undischarged microbasic eurytele (arrow indicates the inverted shaft; scale bar = 3 µm); (*e*) a light micrograph of an undischarged A-isorhiza (scale bar = 3 µm); (*f*) a light micrograph of a small, undischarged a-isorhiza (scale bar = 3 µm); (*g*) a light micrograph of a large undischarged nematocyst, with an unclear tubule pattern (arrow indicates a 'big' operculum; scale bar = 3 µm); (*h*) a light micrograph of an undischarged p-mastigophore (arrow indicates the shaft; scale bar = 3 µm).

(see Fig. 13). Moreover, the results from the combined datasets of morphological and gene sequences (mtDNA, 28S and ITS) gave congruent results with the gene tree (see Fig. 11), placing *Pelagia noctiluca* most distantly from other pelagiid genera, both obtained by Bayesian approach (MrBayes 3.2.1).

Discussion

Morphological differences and phylogenetic analysis together allowed us to separate the recently described species *Pelagia benovici* (Piraino *et al.* 2014) from other genera in the Pelagiidae, and to reclassify this species into the new genus *Mawia*. A phylogenetic analysis of several nuclear and mitochondrial loci, together with morphological data, revealed that *Mawia benovici* is clearly separated from all other investigated genera within Pelagiidae (Fig. 11). A comparison of COI sequences from *M. benovici* revealed low haplotype diversity and gave a clear signal for species delimitation and nuclear markers, especially with the significant region in the 28S rRNA, which pointed out delimitation at genus level. This region is identical for three examined species within genus *Chrysaora*, while it is different between examined genera. These findings are also supported by the comparison of the morphological features of *M. benovici* with the other pelagiid species (*Sanderia malayensis*, *S. pampinosus*, *Pelagia noctiluca* and *Chrysaora* species), of which the main ones at the genus level are synthesised in Table 5. Cladistic analyses of 32 morphological characters (see the Results for the list), considered as unordered, revealed close relationships between *Mawia* and *Chrysaora* (Fig. 13) and confirm the phylogenetic analysis on nuclear and mitochondrial loci, also support separation of new jellyfish from genus *Pelagia*. The present study is one of the rare studies dealing with relationships within genera in Pelagiidae in order to uncover a phylogenetic relationship in spite of main obstacles, such as homoplasies in morphological characters and a paucity of diagnostic characters.

Several morphological diagnostic features (Tables 3, 5, Figs 4–9) enable the re-assignment of the previously described *Pelagia benovici* into the new genus *Mawia*.

The *gastric pouches* are all alike in *Mawia* (Fig. 4*b*), with straight radial septa, thicker proximally with a rounded edge. In *Pelagia* the radial septa are also straight, with the proximal, thicker edge sometimes rounded or teardrop-shaped, but more frequently triangular or T-shaped (both edges can be present in the same specimen irregularly alternating; other specimens only exhibit triangular or T-shaped edges), and the pouches are all alike. In both genera the distal termination is just in the middle of the marginal lappets, equidistant from tentacles and rhopalia. In *Chrysaora*, aside from a certain variability, the radial septa can be straight initially. However, in the distal area they curve towards the rhopalia, then turn again towards the tentacles, and ending into the rhopalar lappets near the tentacular base (Fig. 6*a*) as in *C. hysoscella* and *C. lactea*, thereby enlarging the distal portion of the tentacular pouches (the 'Atlantic pattern,' as

Table 4. Genus-level characters and character states for *Sanderia*, *Mawia*, *Chrysaora*, *Pelagia* and the outgroup (*Cyanea*)

(1) *Umbrella overall shape*: 0 = hemispherical, more or less flattened in the central area; 1 = central disk with an irregular pattern of shallow furrows, honeycomb-like pattern.
(2) *Umbrellar nematocyst warts*, *thickness and protrusion from the umbrellar surface*: 0 = no or weak, faint protrusion; 1 = clear protrusion; 2 = papillar protrusions in the marginal area only.
(3) *Rhopalia*, *number*: 0 = 8; 1 = 16.
(4) *Exumbrellar sensory pits shape of the longitudinal section*: 0 = symmetric isosceles triangle; 1 = right triangle.
(5) *Exumbrellar sensory pits*, *depth*: 0 = shallow; 1 = deep.
(6) *Exumbrellar sensory pits*, *LM ratio*: 0 = less than 0.25; 1 = more than 0.25.
(7) *Exumbrellar sensory pits*, *AS ratio*: 0 = less than 0.5; 1 = more than 0.5.
(8) *Marginal tentacles*, *origin*: 0 = arising from the umbrellar margin; 1 = arising from subumbrellar surface at some distance from the margin.
(9) *Marginal tentacles*, *total number*: 0 = 8; 1 = 16; 2 = number can vary from 8 to 40 or little bit more in different species; 3 = many, more than 50, arranged in eight subumbrellar adradial clusters each consisting in more than one row.
(10) *Marginal tentacles*, *number between adjacent rhopalia*: 0 = 1; 1 = more than 1.
(11) *Marginal tentacles-rhopalia ratio* (*total number*): 0 = 1; 1 = 3, 5 or a few more; 2 = many, more than 10.
(12) *Marginal tentacles*, *basal portion anatomy*: 0 = smooth, without folds or furrows, in one species with a row of vacuoles in the central tentacle only; 1 = with localised longitudinal adaxial ectodermal furrows.
(13) *Marginal tentacles*, *anatomy*: 0 = without mesogleal folds, or adaxial furrow or thickenings; 1 = with an adaxial longitudinal furrow in the mesoglea; 2 = with epidermal longitudinal adaxial thickening; 3 = with epidermal longitudinal muscular folds in the mesoglea, the deeper adaxial.
(14) *Marginal lappets*, *total number*: 0 = 16; 1 = 32; 2 = 32 and more –in different species.
(15) *Marginal lappets*, *shape*: 0 = width and length equivalent or larger than long, with a slight cleft in the middle; 1 = longer than wide.
(16) *Gastrovascular sinus*: 0 = tentacular and rhopalar pouches equal; 1 = tentacular pouches wider throughout their length; 2 = tentacular pouches wider distally; 3 = tentacular and rhopalar pouches equal or slightly wider proximally and distally.
(17) *Presence and shape of gastrovascular protrusions in the marginal lappets*: 0 = present, one per lappet; 1 = present, two extensions in the lateral portions of each marginal lappet; 2 = present or absent, depending on the species, if present 2 protrusions in the lateral portions of the rhopaliar lappet, 1 only in the tentacular; 3 = present, with several irregularly ramified branches in each lappet.
(18) *Tentacular and rhopalar lappets*, *shape*: 0 = equal, symmetric; 1 = equal, asymmetric; 2 = mainly unequal, with rhopalar asymmetric, few species equal.
(19) *Radial septa*, *overall shape*: 0 = straight throughout; 1 = straight throughout or with shallow 'S'-curve in distal 1/4, ending towards rhopalia in different species; 2 = straight proximally, then markedly S-shaped; or straight proximally, then bending towards rhopalia in different species; 3 = straight, with irregular, short lateral branches, wider in the distal portion, sometimes with anastomoses across them which connect the adjacent gastric pouches.
(20) *Radial septa*, *proximal shape*: 0 = rounded, teardrop- or circular-shaped, the thickness of which is reduced sharply just after the origin; 1 = rounded, whose thickness gradually decreases distally; 2 = triangular or rounded - in different species; 3 = mainly circular, but some triangular, irregularly alternating in the same specimens.
(21) *Radial septa*, *distal ending*: 0 = just in the middle of the marginal lappet; 1 = near the tentacle, at the basis of the marginal lappet; 2 = asymmetrically in the marginal lappet, closer to rhopalia, but with the end irregularly turning towards the tentacular portion of lappet.
(22) *Subumbrellar musculature*: 0 = coronal muscle annular, just under the gastric septa, weakly folded, radial muscles not perceptible; 1 = coronal muscle annular, starting before the origin of gastric septa, highly folded circularly, ending distally at about a quarter or a third of the gastric septa total length, with well developed radial muscles starting from the distal margin of coronal muscle, equally folded. Folds can hold rows of pit-like extensions of the gastrovascular sinus.
(23) *Gonads pattern in living specimens*: 0 = four leaf-shaped; 1 = four leaf-shaped or heart-shaped, with protrusion in the subumbrellar papillae; 2 = cross-shaped, with concavity facing outwards; 3 = irregular semicircular ring, with many folds; 4 = highly folded, markedly dangling freely beneath the subumbrella.
(24) *Gonads*, *degree of foldings*: 0 = low, not affecting the overall gonad topography; 1 = high, with protrusion in gonadal papillae, but not affecting the overall gonad topography; 2 = high, affecting the overall gonad topography.
(25) *Gonads*, *finger-shaped papillae*: 0 = absent; 1 = present.
(26) *Gonads*, *nematocyst warts on gonad subumbrellar epidermal outline*: 0 = absent; 1 = present.
(27) *Subgenital ostium*: 0 = absent; 1 = a wide area, bounded by basal pillars laterally and in part distally; 2 = a wide area, bounded by basal pillars laterally and their branches plus a row of papillae distally; 3 = very evident and localised, delimited everywhere from the basal pillars enlargements.
(28) *Basal pillars*, *shape*: 0 = absent; 1 = Y-shaped, slight, lateral distal branches shorter, slightly curved with concavity facing inwards, single arch cross-section; 2 = Slight, elongated rectangular shape, single arch cross-section, lateral edges diverging distally and fused; 3 = Thick or very thick, distally branched, the ends of adjacent branch fused, double arch cross-section, noticeable perradial embayment, sometimes quadralinga in some species; 4 = Slight, roughly trapezoid, larger distally, double arch cross-section, shallow perradial embayment, lateral edges diverging distally.
(29) *Oral arms*, *distal portion*: 0 = not spirally coiled; 1 = spirally coiled.
(30) *Manubrium and oral arms interradial mesogleal layer*: 0 = thin, inconsistent; 1 = thick, solid.
(31) *Manubrium nematocyst warts*: 0 = small, not visible at the naked eye; 1 = large and evident, similar to the umbrellar ones.
(32) *Biological cycle*: 0 = meroplanktonic; 1 = holoplanktonic.

defined by Morandini and Marques 2010). In other species, like *C. fuscescens*, *C. pacifica*, and *C. plocamia* they are straight initially, then 'S'-shaped, first thinning the tentacular pouch, then enlarging it, and ending into the rhopaliar lappet, near the tentacular base (the 'Pacific pattern,' Morandini and Marques 2010). In *Sanderia* the radial septa are straight, with a rounded or teardrop-shaped proximal edge, distal termination just in the middle of the marginal lappets, equidistant from tentacles and rhopaliar, with gastric pouches that are all alike in *S. malayensis*. In *S. pampinosus* Gershwin and Zeidler (2008*b*) describe the distal portion as: 'with a shallow 'S-curve' in the distal 1/4, ending towards rhopalia,' thus widening the tentacular

Table 5. Selected diagnostic morphological features suitable for discriminating Pelagiidae genera

	Sanderia[A]	*Mawia*, gen. nov.	*Chrysaora*[B]	*Pelagia*[C]
Tentacles, rhopalia, marginal lappets, and gastric pouches nr	16; 16; 32; 32	8; 8; 16; 16	8–50; 8; 32 or more; 16	8; 8; 16; 16
Marginal tentacles: origin area	*S. malayensis* in the adaxial area of the tentacle origin there are several, short epidermal tight furrows, which do not extend in the tentacle	Smooth	In the adaxial area adjacent to the tentacle origin there are several, very shallow, short epidermal tight furrows, which do not extend in the tentacle	Smooth
Marginal tentacles: anatomy	*S. malayensis* laterally compressed, *S. pampinosus* ab- adaxially compressed. Without mesogleal folds, or adaxial furrow or thickenings	Laterally compressed, without mesogleal folds, or adaxial furrow or thickenings	Ribbon-like proximally, with an adaxial longitudinal furrow in the mesoglea, at least in the basal (proximal) part	With epidermal longitudinal muscular folds in the mesoglea, the deeper adaxial
Basal pillars	Slight, elongated rectangular shape, single arch cross-section, lateral edges diverging distally, continuing under the gonads and then merging with the adjacent edge	Y-shaped, slight, lateral distal branches shorter, slightly curved with concavity facing inwards, single arch cross-section, proximal portion thicker, right triangle-shaped if observed laterally	Thick or very thick, distally branched, the ends of adjacent branch more or less fused, double arch cross-section, noticeable perradial embayment, sometimes quadralinga	Slight, roughly trapezoid, larger distally, double arch cross-section, shallow perradial embayment, lateral edges diverging distally
Radial septa	Straight, with teardrop-shaped proximal edge, with gastric pouches all alike (*S. malayensis*) or with slight S-shaped distal portion, with larger tentacular pouches (*S. pampinosus*), distal end symmetric between rhopalia and tentacles, or closer to rhopalia	Straight, with rounded proximal edge, with gastric pouches all alike, distal end symmetric between rhopalia and tentacles	With proximal straight portion, with rounded to triangular proximal edge, and S-shaped distal portion, with larger tentacular pouches, distal end generally closer to tentacles	Straight, with sometimes rounded proximal edge, more frequently triangular or T-shaped, with gastric pouches all alike, distal end symmetric between rhopalia and tentacles
Gonads pattern	Horseshoe-shaped, with external pendant hollow papillae containing gonad folds, lateral portions not beneath basal pillars, covered by nematocyst warts	Horseshoe simple folded ribbon-like, with concavity facing the manubrium, slightly protruding; covered by nematocyst warts	Extremely folded, highly protruding from the subgenital pouch, lateral portions beneath basal pillars	Ribbon-like strongly folded, protruding from the subgenital pouch, lateral portions beneath basal pillars. In living specimens tend to be arranged into a cruciform shape (median area shifted near the manubrium)
Subgenital ostium	Wide flat area, heart-shaped in *S. malayensis*, horseshoe-shaped in *S. pampinosus*, laretally and distally delimited by the gonads plus papillae	Wide flat area, clover-shaped, gonad foldings slightly protruding in the distal area	Very evident, broad to narrow, of variable shape from circular to heart-shaped, etc., from which gonad folding may protrude	Wide flat area, seed to barrel shaped, distally containing the protruding gonadic foldings
Exumbrellar sensory pits	Small, shallow, ovoid-ellipsoid, with the deepest point central, longitudinal section like a flattened isosceles triangle*	Shallow, ovoidal, of glass-like transparency, longitudinal section as a right triangle, with the minor cathetus (facing outwards) ~1/3 of the larger cathetus	Deep, generally ovoidal to ellipsoidal, longitudinal section like an elongated cone with the apex curved outwards	Shallow, ovoid-ellipsoid, with the deepest point central, longitudinal section like a flattened isosceles triangle
Sensory pits:LM and AS ratio	0.25 and 0.49	0.28 and 0.24	0.50 and 0.23	0.24 and 1.10

[A]Data from: present work and Goette, 1886, Mayer, 1910, Kramp, 1961, Franc, 1993, Gershwin and Zeidler, 2008b, Morandini and Marques, 2010 and * Avian, pers. observations.

[B]Data from: present work and Mayer, 1910, Kramp, 1961, Russell, 1970, Gershwin and Collins, 2002, Gershwin and Zeidler, 2008a, Morandini and Marques, 2010.

[C]Data from: present work and Mayer 1910, Kramp 1961, Russell 1970, Gershwin and Collins 2002, Gershwin and Zeidler 2008*a*, Morandini and Marques 2010.

Table 6. Evolutionary divergence across mitochondrial loci (COI, 16S, 12S) and nuclear loci (28S, ITS1, ITS2) between *Mawia benovici* and *Pelagia noctiluca*, *Chrysaora hysoscella*, and *Sanderia malayensis* (top), and within species in Pelagiidae (bottom)

Distances based on the Kimura-2-parameter model, presented together with standard errors

Species	*Mawia benovici* to other species in Pelagiidae (d ± s.e.)					
	COI	16S	12S	28S	ITS1	ITS2
Pelagia noctiluca	0.399 ± 0.043	0.269 ± 0.028	0.217 ± 0.027	0.125 ± 0.016	0.367 ± 0.052	0.241 ± 0.031
Chrysaora hysoscella	0.380 ± 0.040	0.128 ± 0.019	0.114 ± 0.018	0.148 ± 0.017	0.439 ± 0.067	0.267 ± 0.032
Sanderia malayensis	0.290 ± 0.033	0.072 ± 0.013	No data	0.104 ± 0.013	No data	No data
	Evolutionary divergence within species in Pelagiidae (d ± s.e.)					
Species	COI	16S	12S	28S	ITS1	ITS2
Mawia benovici	0.000 ± 0.000	0.006 ± 0.002	0.000 ± 0.000	0.003 ± 0.001	0.004 ± 0.002	0.002 ± 0.001
Pelagia noctiluca	0.035 ± 0.005	0.008 ± 0.002	0.011 ± 0.003	0.003 ± 0.001	0.004 ± 0.001	0.004 ± 0.002
Chrysaora hysoscella	0.005 ± 0.004	0.005 ± 0.002	0.066 ± 0.013	0.001 ± 0.001	0.001 ± 0.001	0.000 ± 0.000
Sanderia malayensis	[A]	0.017 ± 0.005	No data	[A]	No data	No data

[A]Only 1 sequence.

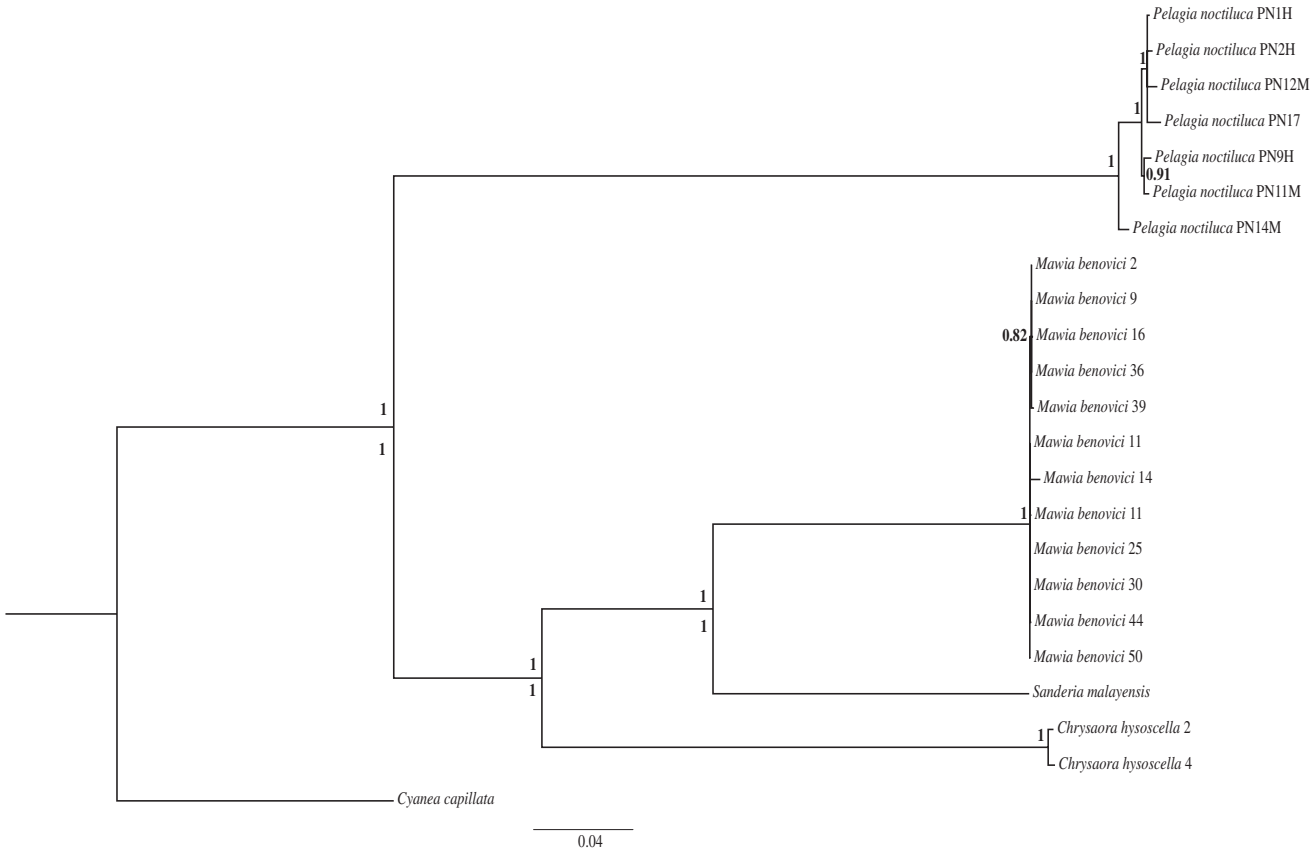

Fig. 11. Phylogenetic relationships between *Mawia benovici*, *Pelagia noctiluca*, *Sanderia malayensis*, *Chrysaora hysoscella* and *Cyanea capillata* inferred from concatened sequences of six loci dataset (COI-16S-12S-28S-ITS1-ITS2) analysed together with morphological characters by the Bayesian approach (numbers at nodes indicate posterior probability: above the line for gene tree and below line combined analysis).

pouches. Unfortunately, this description is solely based on three specimens collected in 1982, and one of them was damaged (Gershwin and Zeidler 2008*b*), without pictures or drawings. The extensions of the gastric pouches inside the marginal lappets, although the margin can be irregular, are more rounded in *Mawia benovici* (Figs 3, 4*b*, *d*) than those of *P. noctiluca* (Russell 1970: 74, fig. 38). A similar pattern to that of *Mawia benovici* can be observed within the genus *Chrysaora*, for example *C. colorata*

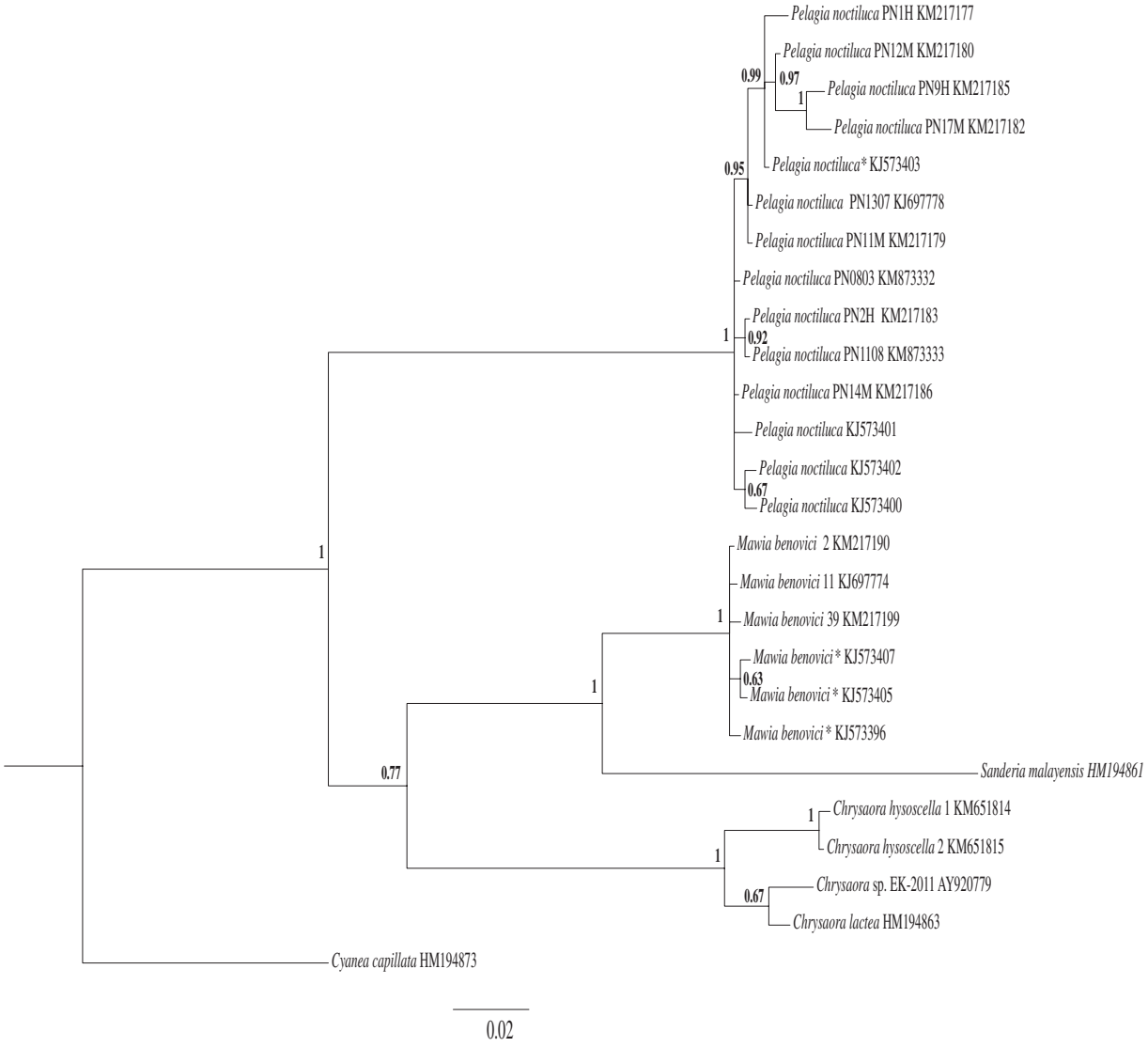

Fig. 12. Phylogenetic relationships between *Mawia benovici*, *Pelagia noctiluca*, *Sanderia malayensis*, *Chrysaora* spp. and *Cyanea capillata* based on 28S rDNA inferred by the Bayesian approach (numbers at nodes indicate posterior probability).

Russel, 1964 (Morandini *et al.* 2004; Morandini and Marques 2010). In *Sanderia malayensis* these extensions are similar to those observed in *Mawia* and described as triangular-shaped in *S. pampinosus* (Gershwin and Zeidler 2008*b*).

The pattern of the *exumbrellar nematocyst warts* of *Mawia benovici* differs from that of *P. noctiluca*, the latter has larger, irregularly shaped, and more dispersed warts in adults. The shape of the *M. benovici* larger warts in the umbrellar central area is not equivalent with the larger and thicker papillar warts present in the genus *Sanderia* (Gershwin and Zeidler 2008*b*). In *Chrysaora* the warts shape, size, and colouration are too variable to make affordable comparisons (Morandini and Marques 2010).

The *umbrellar colour pattern* of *M. benovici*, rather than *P. noctiluca*, is more similar to at least some species of *Chrysaora*, e.g. younger specimens of *C. hysoscella*, except for the star-shaped (compass) exumbrellar marks, which, however, develop only in adult specimens, but with a wide variability – from totally absent to very evident (Russell 1970; Morandini *et al.* 2004; Morandini and Marques 2010). *Sanderia malayensis* is sometimes described as pale yellowish (Mayer 1910; Kramp 1961), while all the specimens observed in the present study were completely colourless.

The exumbrellar *sensory pit* of *Mawia benovici* (Table 5, Fig. 7*b*, *d*) exhibits some peculiarities: its longitudinal section is approximately right triangle-shaped, with the deepest tip near the distal margin, with a mean LM ratio of 0.28, and a mean AS ratio of 0.24 ($n = 4$), like in *Chrysaora hysoscella* (Fig. 8*a*, *c*), with a mean LM ratio of 0.507 and a mean AS ratio of 0.23, $n = 5$; sometimes with the deepest tip slightly curved outwards. It is not like an isosceles triangle, as in *Pelagia* (Fig. 8*b*, *d*), with a mean LM ratio of 0.24 and a mean AS ratio of 1.10 ($n = 5$), or a deep, elongated curved cone with the tip facing outwards, as in other species of the genus *Chrysaora* (Bigelow 1910; Russell 1970; Gershwin and Collins 2002; Morandini and Marques

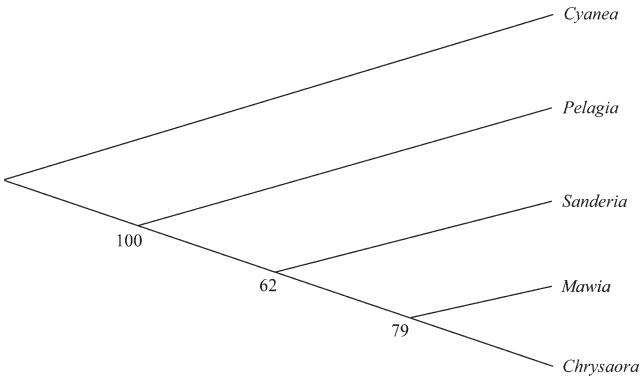

Fig. 13. Maximum parsimony tree of morphological characters obtained by branch-and-bound search using the cladistics option in PAST V2.17. The tree with best bootstrap values based on genus level morphological characters from Table 3, characters treated as unordered and 500 bootstrap replicates were used.

2010). In *Sanderia malayensis* (Fig. 7*a*, *c*) the sensory pits are like an isosceles triangle, similar to those observed in *P. noctiluca*, with the deepest tip slightly shifted towards the umbrellar margin with a mean LM ratio of 0.25, and a mean AS ratio of 0.49 ($n = 3$). To our knowledge, no data about sensory pits in *S. pampinosus* are available. Furthermore, the genus *Sanderia* is unique within all the Semaeostomeae for the fact of possessing 16 rhopalia. In *M. benovici* there is also a peculiar glass-like transparency that can be easily detected by the naked eye both in living and in freshly preserved specimens (Fig. 4*d*, *e*). This transparency is due to the underlying less opaque mesogleal layer. Nematocyst warts, well pigmented, are present on the distal edge of the sensory pit (Fig. 7*b*), and surround the sensory pit area.

The shape of *manubrium* of *Mawia benovici* is more similar to at least some species of the genus *Chrysaora* than to *Pelagia noctiluca*. Its peculiar characteristics are the shortness of the proximal, undivided portion, and the particular weakness and softness of the mesogleal layer (Fig. 9*d*, *e*), unlike the robustness in the manubrium of *P. noctiluca* (Fig. 9*f*). In *Sanderia* the manubrium has a long and tubular proximal portion (Vanhöffen 1902; Franc 1993; Gershwin and Zeidler 2008*b*), unlike that of *M. benovici*. In *Chrysaora* its length is variable, from well developed to very short (Morandini and Marques 2010).

The *oral arm frillings* in *Mawia benovici* (Figs 2*c*, 9*d*, *e*) are more developed than in *P. noctiluca* (Fig. 9*f*), even if not so elongated, flown, and distally coiled as those of *C. hysoscella*. In *Sanderia* there are long, frilled oral arms with small warts (Vanhöffen 1902; Franc 1993; Gershwin and Zeidler 2008*b*), undetectable in *M. benovici*.

The epidermal muscular folds within the mesogleal layer are absent in the *marginal tentacles* of *Mawia benovici* (Fig. 5*b*, *d*) and was considered as a species-specific character by Piraino *et al*. (2014). This characteristic is completely different in *Pelagia noctiluca* (Fig. 6*b*, *d*). Data on tentacle cross-sections in other genera are scarce, apart from two *Chrysaora* species, *C. quinquecirrha* (Desor, 1848) (Burnett and Sutton 1969) and *C. hysoscella* (Fig. 6*a*, *c*). Russell (1970) indicated an adaxial (subumbrellar) longitudinal furrow in the basal portion (or bulb) of tentacles in *Chrysaora*. Our observations in *C. fuscescens*, *C. hysoscella*, *C. lactea*, *C. pacifica*, and *C. plocamia* confirm the presence of this furrow. Close to the tentacle origin there are several, very shallow, short subumbrellar epidermal tight furrows, which however do not extend in the tentacle basis (Fig. 6*a*). Apart the proximal adaxial furrow, the tentacles' histology is very similar to that observed in *M. benovici*. In *Sanderia malayensis* the epidermal muscular folds within the tentacular mesogleal layer are absent, as well as an adaxial furrow (Fig. 5*c*), but there is a peculiarity: in the adaxial area of the tentacle origin there are several, short epidermal tight furrows, which do not extend in the tentacle (Fig. 5*a*). Their number increase with the size of the jellyfish. No data are available on *Sanderia pampinosus* tentacles, apart their ab-adaxial compression (Gershwin and Zeidler 2008*b*). In this context, we suggest that the tentacle anatomy has to be considered a genus-specific character within Pelagiidae: the simplest form, like the tentacles of *Mawia* being a primitive, plesiomorphic trait, and the most complex, as observed in *Pelagia*, the derived (apomorphic) trait.

The structure of *basal pillars* in *Mawia benovici* (Figs 3, 4*c*), as described in the Results, is different from that of the well known *P. noctiluca* (Table 5). *Chrysaora* exhibits a wide variability in this characteristic (Russell 1970; Gershwin and Zeidler 2008*a*; Morandini and Marques 2010), and is always different from that observed in *M. benovici*. The basal pillars of *Sanderia* are not thick, with an elongated rectangular shape, single arch cross-section, with lateral edges diverging distally and fused, thus forming a thickening just under the gonads in immature specimens, from which subsequently develop gonadal papillae.

The *gonad topographic pattern* of *Mawia benovici* is horseshoe-shaped, precisely interposed between the basal pillars, with simple foldings and only protruding slightly into the interradial area. The sides of the gonads do not protrude below the pillars ever (Figs 3, 4*c*, 9*a*), but neatly follow the lateral edges, unlike *Pelagia* or *Chrysaora*, but similarly to *Sanderia*, at least in *S. pampinosus* (Gershwin and Zeidler 2008*b*). In *S. malayensis* the gonad pattern is described as heart-shaped (Goette 1886; Vanhöffen; 1902; Mayer 1910; Kramp 1961; Franc 1993; Gershwin and Zeidler 2008*b*), even if the gonadic pattern in immature specimens we observed is horseshoe-shaped. The gonads in *M. benovici* are covered by nematocyst warts, and do not match either *Pelagia* or *Chrysaora* (Figs 2, 3, 4*i*), but match *Sanderia*, whose papillae are covered by nematocyst warts, as well (Gershwin and Zeidler 2008*b*). In *S. malayensis* immature specimens the overall pattern is closer to that observed in *Mawia* nematocyst warts included. Overall, the gonad arrangement in *M. benovici* more resembles those present in Semaeostomeae juvenile stages, at the beginig of gonads development. In *Sanderia*, it is possible to observe an increase in the degree of folds that are housed in the gonadal papillae, whose presence is a distinctive feature of this genus. In *Pelagia*, there is a further increase of the folds, accompanied by a hypertrophy of the subumbrellar gastrodermis, especially in the interradial area. In living medusae this allows the gonads to shift towards the manubrium, thereby obtaining the typical cruciform gonadic pattern. In *Chrysaora*, the degree of folds is much greater, again accompanied by a hypertrophy of the

subumbrellar gastrodermis, so the convolutions of the gonad are extremely complicated, sometimes with an overall arch pattern, whose concavity faces outwards.

There is a vague resemblance with *Discomedusa lobata* Claus, 1877 (more) and *Aurelia* sp.8 (*sensu* Dawson *et al.* 2005) (less) gonads, where otherwise is a well developed subgenital pit (or pouch). The spermatic follicles' histological structure in *Mawia* is similar to those detected in some other scyphozoans, like *Pelagia noctiluca*, *Aurelia* sp.8 or *Discomedusa lobata* (Rottini Sandrini *et al.* 1986; Avian and Rottini Sandrini 1991; Avian *et al.* 1991*b*; Rottini Sandrini and Avian 1991) and *Chrysaora hysoscella* (Widersten 1965; Avian, unpubl. data). No data are available for *Sanderia*.

The *subgenital ostium* area of *Mawia* is completely different to those present in the genus *Chrysaora* (Gershwin and Collins 2002; Morandini and Marques 2010). In *Pelagia*, it is more enlarged, but not like in *Mawia benovici* specimens, and is more restricted distally, due to the different shape of the oral pillars. In *Sanderia* there seem to be differences between *S. malayensis* and *S. pampinosus* (Gershwin and Zeidler 2008*b*), but in both species the presence of gonadal papillae makes the subgenital area different from that present in *Mawia*. The gonads colouration in living *Mawia* specimens is ivory white/pale sandy. In addition, the reexamination of the Holotype and Paratype I (currently the only specimen defined as female) showed similar ivory white/pale sandy colour, whilst taking account of the discolouration due to formaldehyde preservation. The comparison with the *Mawia* pictures from November 2004 (Fig. 2*d*), depicting some specimens with intensely-coloured gonads may indicate that this apparent colour differences are related to the ovaries maturation stage, still immature in September (light colour, not dissimilar to the testes), but which could be fully developed in November.

Gershwin and Collins (2002) pointed out the problems about lack of systematics studies in Pelagiidae, basically relying only on few morphological features. They also pointed to the problem in identifying a suitable outgroup to infer pelagiid phylogeny, and to identify the true direction of character changes. The use of independent genetic markers ensures robust analysis in taxonomy, especially when describing cryptic species (Pante *et al.* 2015*b*; Jörger and Schrödl 2013). Availability of credible gene markers for species delimitation is of crucial importance considering the complexity of scyphozoans taxonomy and were justified in several studies of scyphozoan phylogeny (Collins 2002; Collins *et al.* 2006). In our study, a phylogenetic analysis of reliable genetic markers which have a different mode of inheritance and different rate of substitutions were used to resolve the taxonomic position and phylogenetic relationships of the recently discovered species *Mawia benovici* within Pelagiidae. The phylogenetic analyses included all the valid genera within Pelagiidae (*Pelagia*, *Sanderia* and *Chrysaora*). Morphological characters were considered unordered in the cladistic analysis also due to many unresolved homoplasies and unknown evolution of characteristics. The most parsimonious tree does not support a close relationship between *Pelagia* and *Mawia benovici*, but a closer relationship with *Chrysaora* (Fig. 13), while the phylogenetical analysis done with sequences and morphological characters together (Fig. 11) confirmed a closer relationship between *Mawia* and *Sanderia*. The previously mentioned obstacle, related with evolution of characters, might be more evident in the results of the cladistic analysis and less pronounced in combined analysis supporting relationships between *Mawia* and *Sanderia.*

The phylogenetic inference (using the Bayesian approach and ML) of *Mawia benovici* by using nuclear 28S rRNA, ITS1/ITS2 regions and mitochondrial genes COI, 16S and 12S with different evolutionary rates positioned this species as the sister species with *Sanderia malayensis* (Fig. 11 and Supplementary Material 5). *M. benovici* and *S. malayensis* shared the most recent common ancestor with *Chrysaora hysoscella*. Phylogenetic analysis of nuclear gene 28S rRNA did not reveal any sign of hybridisation between *Mawia benovici* and *Pelagia noctiluca*, which contradict the previous hypothesis in Piraino *et al*. (2014). Our analysis revealed that 28S rRNA sequences of Pelagiidae provide diagnostic characteristics for each considered genus (Fig. 12). These diagnostic characters allowed us to re-classify all the available 28S rRNA sequences for *Mawia benovici* (see Table 2). Manual alignment of 28S rRNA sequences revealed indels with diagnostic values related with examined genera in Pelagiidae: *Mawia benovici* has GAAG, *Chrysaora hysoscella*, *Chrysaora lactea* and *Chrysaora* sp. have GAGA, *Sanderia malayensis* has GCGG, while in *Pelagia noctiluca* there is a deletion at this site. Very low polymorphism was found in the analysed nuclear and mitochondrial markers of *M. benovici*, which reveals a very genetically homogenous population (see Table 6). Biological mechanisms for homogenising 28S rRNA sequences were well described in several taxa. Most taxa harbor one ribosomal cluster because of concerted evolution (Elder and Turner 1995; Markmann and Tautz 2005). Very little intra-individual polymorphism was found in the D1–D2 region of 28S rRNA (Sonnenberg *et al.* 2007), which is also the case of *M. benovici*. Nevertheless, this region D1–D2 is suitable to distinguish congeneric species (Verheyen *et al.* 2003; Sonnenberg *et al.* 2007). The characteristic of this marker is also the length variability due to indels, which can provide additional information for species discrimination belonging within Pelagiidae. For all these reasons, we used polymorphism in the 28S rRNA sequences in *M. benovici* as a diagnostic character at the genus level. Therefore, nuclear locus 28S rRNA proved to be a good marker for phylogenetic inference in the medusozoan (Collins *et al.* 2006), and showed to be useful for the delimitation and for inference of relationships between *Mawia benovici* and the other members of Pelagiidae.

In some studies, 16S enabled a high degree of differentiation among scyphozoans (Schroth *et al.* 2002; Collins *et al.* 2006; Bayha *et al.* 2010). The use of this marker for *Mawia benovici*, confirmed the separation of this species from other pelagiid species. Taking into consideration the different mode of evolution of nuclear ribosomal genes compared with COI, and that COI and 16S are mitochondrial, and thus more prone to mutations (Kayal *et al.* 2012), all analysed genes supported *Mawia benovici* as a separate group. The same results were achieved by the cladistic analysis of the morphological characters (Fig. 13) and the the combined analysis with the gene tree (Fig. 11).

Several measures of polymorphism (haplotype diversity (h), nucleotide diversity (π) and genetic distances) pointed out that

the investigated population of *Mawia benovici* is extremely genetically impoverished (for COI $h = 0.116$, $\pi = 0.0022$). This is strikingly opposite to *Pelagia noctiluca*, where high diversity among COI haplotypes ($h = 0.963$, $\pi = 0.68$) was found, as previously described by Stopar *et al*. (2010) and likewise in *Rhizostoma pulmo* (Macri, 1778) (Ramšak *et al.* 2012). A comparison of genetic distances as a measure of substitutions per site in haplotypes revealed the smaller distance between *Mawia benovici* and *Sanderia malayensis* at COI, 16S and 28S loci. The calculated distances in COI (Table 6) between *Mawia benovici* and *Sanderia malayensis* is 0.290 ± 0.033 and is a higher than usually accepted level for species separation. In addition, in *Mawia benovici* intraspecific variability was very low or even zero across all loci. Among Pelagiidae the evolutionary divergence within species at COI locus was the highest in *Pelagia noctiluca*, as already previously estimated (Stopar *et al.* 2010). Higher genetic diversity was also estimated in *Aurelia* sp. 8 and *Rhizostoma pulmo* (Ramšak *et al.* 2012). These results raised the idea that, at the time of our sampling, the population of *Mawia benovici* was extremely genetically impoverished. In turn, this could suggest that, if introduced, as suggested by Piraino *et al*. (2014) only a few specimens of *Mawia benovici* arrived in the Adriatic Sea and, as consequence, the sampled specimens could derive from the reproduction of a very few number of individuals or polyps (founder effect). Conversely, if *Mawia benovici* was present in the deeper water of the Adriatic Sea (as never previously observed along the coast), we could attribute its genetic impoverishment to a severe genetic drift.

Another intriguing question, still to be resolved, is related to the observed sex ratio (female scarcity) in our samples. If *Mawia benovici* will reappear, as we hope, future observations will likely help us to understand its origin and future research will primarily focus on its biological cycle. Moreover, we hope that in near future more combined morphological and genetic analyses of multiple species of each pelagiid genus will verify the robustness of the original genera description and phylogeny.

Acknowledgements

This study was financed by the project PERSEUS (Policy-oriented marine Environmental Research for the Southern European Seas, FP7 contract number 287600), the Italian Flagship Project RITMARE (Ricerche Italiane sul Mare), the Project MEDIAS (EU Mediterranean Coordinated Survey on Small Pelagic), and Slovenian research program P1–0237. We wish to thank M. Bastianini, D. Borme, G. Coidessa, P. Del Negro, J. Francé, A. Goruppi, T. Juretić, A. Nella, the staff of the Osservatorio Alto Adriatico Arpa FVG, the CNR-ISMAR research group working on the small pelagic acoustic survey in the Adriatic, and the crew of the RV G. Dalla Porta for their help in providing observations and samples of *Mawia benovici*; M. Pansera for samples of *P. noctiluca* from the Strait of Messina; and S. N. Stampar kindly provided sequences of *Sanderia malayensis* (FAPESP - 12/01771–8). L. Prieto (CSIC, Spain), M. Vodopivec (MBS-NIB) provided *Pelagia* samples from the SOCIB expedition in 2014, and D. Angel (University of Haifa) kindly provided fresh samples of *P. noctiluca* from the eastern Mediterranean. Our thanks go to T. Makovec (MBS-NIB) for the photographs of *M. benovici* from November 2004; and A. Weissenbacher (Schönbrunner Tiergarten, Vienna, Austria) for providing a clip of *M. benovici* and specimens of *Chrysaora fuscescens* and *Sanderia malayensis*. Tatsuo Murakami (Kamo aquarium, Japan), provided specimens of *C. pacifica* and *S. malayensis*; André C. Morandini (Departamento de Zoologia, Instituto de Biociências, Sao Paulo, Brasil), provided specimens of *C. lactea* and *C. plocamia*. We wish to thank R. Poggi (Natural History Museum of Genova) and A. Colla (Natural History Museum of Trieste) for their help with zoological nomenclature; C. Scotti and P. Fiorentino (Library of the Stazione Zoologica in Naples) for their help with bibliographic references, and A. Pallavicini, (Life Science Dept. (DSV), University of Trieste) and P. Trontelj (University of Ljubljana) for their helpful suggestions on the manuscript. We wish to thank the anonymous reviewers, whose comments greatly improved the manuscript.

References

Avian, M., and Rottini Sandrini, L. (1991). Oocyte development of four species of scyphomedusae in the northern Adriatic Sea. *Hydrobiologia* **216/217**, 189–195. doi:10.1007/BF00026461

Avian, M., Del Negro, P., and Rottini Sandrini, L. (1991*a*). A comparative analysis of nematocysts in *Pelagia noctiluca* and *Rhizostoma pulmo*, North Adriatic Sea. *Hydrobiologia* **216/217**, 615–621. doi:10.1007/BF00026521

Avian, M., Giorgi, R., and Rottini Sandrini, L. (1991*b*). Seasonal influence on the vitellogenesis of *Pelagia noctiluca* in Northern Adriatic Sea. *MAP Technical Reports Series* **47**, 22–31.

Avian, M., Spanier, E., and Galil, B. S. (1995). Nematocysts of *Rhopilema nomadica* (Scyphozoa: Rhizostomeae), an immigrant jellyfish in the Eastern Mediterranean. *Journal of Morphology* **224**, 221–231. doi:10.1002/jmor.1052240211

Bastian, T., Lilley, M. K. S., Beggs, S. E., Hays, G. C., and Doyle, T. K. (2014). Ecosystem relevance of variable jellyfish biomass in the Irish Sea between years, regions and water types. *Estuarine, Coastal and Shelf Science* **149**, 302–312. doi:10.1016/j.ecss.2014.08.018

Bayha, K. M., Dawson, M. N., Collins, A. G., Barbeitos, M. S., and Haddock, S. H. D. (2010). Evolutionary relationships among scyphozoan jellyfish families based on complete taxon sampling and phylogenetic analyses of 18S and 28S ribosomal DNA. *Integrative and Comparative Biology* **50**, 436–455. doi:10.1093/icb/icq074

Bigelow, R. P. (1910). A comparison of the sense-organs in medusae of the family Pelagidae. *The Journal of Experimental Zoology* **9**, 751–785. doi:10.1002/jez.1400090404

Boero, F. (2010). The study of species in the era of biodiversity: a tale of stupidity. *Diversity (Basel)* **2**, 115–126. doi:10.3390/d2010115

Burnett, J. W., and Sutton, J. S. (1969). The fine structural organization of the sea nettle fishing tentacle. *The Journal of Experimental Zoology* **172**, 335–348. doi:10.1002/jez.1401720308

Collins, A. G. (2002). Phylogeny of Medusozoa and the evolution of cnidarian life cycles. *Journal of Evolutionary Biology* **15**, 418–432. doi:10.1046/j.1420-9101.2002.00403.x

Collins, A. G., Schuchert, P., Marques, A. C., Jankowski, T., Medina, M., and Schierwater, B. (2006). Medusozoan phylogeny and character evolution clarified by new large and small subunit rDNA data and an assessment of the utility of phylogenetic mixture models. *Systematic Biology* **55**, 97–115. doi:10.1080/10635150500433615

Darriba, D., Taboada, G. L. R., and Posada, D. (2012). jModelTest 2: more models, new heuristics and parallel computing. *Nature Methods* **9**, 772. doi:10.1038/nmeth.2109

Dawson, M. N. (2005*a*). *Cyanea capillata* is not a cosmopolitan jellyfish: morphological and molecular evidence for *C. anaskala* and *C. rosea* (Scyphozoa: Semaeostomeae: Cyaneidae) in south-eastern Australia. *Invertebrate Systematics* **19**, 361–370. doi:10.1071/IS03035

Dawson, M. N. (2005*b*). Renaissance taxonomy: integrative evolutionary analyses in the classification of Scyphozoa. *Journal of the Marine Biological Association of the United Kingdom* **85**, 733–739. doi:10.1017/S0025315405011641

Dawson, M. N., Gupta, A. S., and England, M. H. (2005). Coupled biophysical global ocean model and molecular genetic analyses identify multiple introductions of cryptogenic species. *Proceedings of the National*

Academy of Sciences of the United States of America **102**, 11 968–11 973. doi:10.1073/pnas.0503811102

Elder, J. F., and Turner, B. J. (1995). Concerted evolution of repetitive DNA sequences in eukaryotes. *The Quarterly Review of Biology* **70**, 297–320. doi:10.1086/419073

Folmer, O., Black, M., Hoeh, W., Lutz, R., and Vrijenhoek, R. (1994). DNA primers for amplification of mitochondrial cytochrome c oxidase I subunit from diverse metazoan invertebrates. *Molecular Marine Biology and Biotechnology* **3**, 294–299.

Franc, A. (1993). Classe des Scyphozoaires. In 'Traité de Zoologie. Anatomie, systématique, biologie. Vol. 3. Cnidaires, Cténaires'. (Ed. D. Doumenc.) pp. 597–884. (Masson: Paris.)

Gershwin, L.-A., and Collins, A. G. (2002). A preliminary phylogeny of Pelagiidae (Cnidaria, Scyphozoa), with new observations of *Chrysaora colorata* comb. nov. *Journal of Natural History* **36**, 127–148. doi:10.1080/00222930010003819

Gershwin, L.-A., and Zeidler, W. (2008*a*). Some new and previously unrecorded Scyphomedusae (Cnidaria: Scyphozoa) from southern Australian coastal waters. *Zootaxa* **1744**, 1–18. doi:10.11646/zootaxa.1744.1.1

Gershwin, L.-A., and Zeidler, W. (2008*b*). Two new jellyfishes (Cnidaria: Scyphozoa) from tropical Australian waters. *Zootaxa* **1764**, 41–52.

Goette, A. (1886). Verzeichniss der Medusen, velche von Dr. Sander, Stabsarzt auf S.M.S. "Prinz Adalbert" gesammelt wurden. *Sitzungberichte der Königlich Preussischen Akademie der Wissenschaften zu Berlin* **7**, 831–837.

Hammer, Ø., Harper, D. A. T., and Ryan, P. D. (2001). PAST: Paleontological Statistics Software Package for Education and Data Analysis. *Palaeontologia Electronica* **4**, 4.

Holst, S., and Laakmann, S. (2014). Morphological and molecular discrimination of two closely related jellyfish species, *Cyanea capillata* and *C. lamarckii* (Cnidaria, Scyphozoa), from the northeast Atlantic. *Journal of Plankton Research* **36**, 48–63. doi:10.1093/plankt/fbt093

Jörger, K. M., and Schrödl, M. (2013). How to describe a cryptic species? Practical challenges of molecular taxonomy. *Frontiers in Zoology* **10**, 59. http://www.frontiersinzoology.com/content/10/1/59. doi:10.1186/1742-9994-10-59

Katoh, K., and Standley, D. M. (2013). MAFFT Multiple Sequence Alignment Software Version 7: improvements in performance and usability. *Molecular Biology and Evolution* **30**, 772–780. doi:10.1093/molbev/mst010

Kayal, E., Bentlage, B., Collins, A. G., Kayal, M., Pirro, S., and Lavrov, D. V. (2012). Evolution of linear mitochondrial genomes in medusozoan cnidarians. *Genome Biology and Evolution* **4**, 1–12. doi:10.1093/gbe/evr123

Kocher, T. D., Thomas, W. K., Meyer, A., Edwards, S. V., Pääbo, S., Villablanca, F. X., and Wilson, A. C. (1989). Dynamics of mitochondrial DNA evolution in animals: amplification and sequencing with conserved primers. *Proceedings of the National Academy of Sciences of the United States of America* **86**, 6196–6200. doi:10.1073/pnas.86.16.6196

Kramp, P. L. (1961). Synopsis of the medusae of the world. *Journal of the Marine Biological Association of the United Kingdom* **40**, 7–469. doi:10.1017/S0025315400007347

Librado, P., and Rozas, J. (2009). DnaSP v5: a software for comprehensive analysis of DNA polymorphism data. *Bioinformatics* **25**, 1451–1452. doi:10.1093/bioinformatics/btp187

Mariscal, R. N. (1974). Nematocysts. In 'Muscatine. Coelenterate Biology'. (Eds L. Lenhoff and H. M. Lenhoff.) pp. 129–178. (Academy Press: New York.)

Markmann, M., and Tautz, D. (2005). Reverse taxonomy: an approach towards determining the diversity of meiobenthic organisms based on ribosomal RNA signature sequences. *Philosophical Transactions of the Royal Society of London. Series B, Biological Sciences* **360**, 1917–1924. doi:10.1098/rstb.2005.1723

Marques, A. C., and Collins, A. G. (2004). Cladistic analysis of Medusozoa and cnidarian evolution. *Invertebrate Biology* **123**, 23–42. doi:10.1111/j.1744-7410.2004.tb00139.x

Mayer, A. (1910). 'Medusae of the World – The Scyphomedusae.' (Carnegie Institution: Washington, DC.)

Meyer, C. P., and Paulay, G. (2005). DNA barcoding: error rates based on comprehensive sampling. *PLoS Biology* **3**(12), e422. doi:10.1371/journal.pbio.0030422

Miller, M. A., Pfeiffer, W., and Schwartz, T. (2010). Creating the CIPRES Science Gateway for inference of large phylogenetic trees. In 'Proceedings of the Gateway Computing Environments Workshop (GCE), 14 Nov. 2010. New Orleans'. pp. 1–8.

Morandini, A. C., and Marques, A. C. (2010). Revision of the genus *Chrysaora* Péron and Lesueur, 1810 (Cnidaria: Scyphozoa). *Zootaxa* **2464**, 1–97.

Morandini, A. C., da Silveira, F. L., and Jarms, G. (2004). The life cycle of *Chrysaora lactea* Eschscholtz, 1829 (Cnidaria, Scyphozoa) with notes on the scyphistoma stage of three other species. *Hydrobiologia* **530–531**(1–3), 347–354. doi:10.1007/s10750-004-2694-0

Nei, M., and Kumar, S. (2000). 'Molecular Evolution and Phylogenetics.' (Oxford University Press.)

Östman, C. (2000). A guideline to nematocyst nomenclature and classification, and some notes on the systematic value of nematocycts. *Scientia Marina* **64**, 31–46.

Östman, C., and Hydman, J. (1997). Nematocyst analysis of *Cyanea capillata* and *Cyanea lamarckii* (Scyphozoa, Cnidaria). *Scientia Marina* **61**, 313–344.

Pante, E., Puillandre, N., Viricel, A., Arnaud-Haond, S., Aurelle, D., Castelin, M., Chenuil, A., Destombe, C., Forcioli, D., Valero, M., Viard, F., and Samadi, S. (2015*a*). Species are hypotheses: avoid connectivity assessments based on pillars of sand. *Molecular Ecology* **24**, 525–544. doi:10.1111/mec.13048

Pante, E., Schoelinck, C., and Puillandre, N. (2015*b*). From integrative taxonomy to species description: one step beyond. *Systematic Biology* **64**, 152–160. doi:10.1093/sysbio/syu083

Piraino, S., Aglieri, G., Martell, L., Mazzoldi, C., Melli, V., Milisenda, G., Scorrano, S., and Boero, F. (2014). *Pelagia benovici* sp. nov. (Cnidaria, Scyphozoa): a new jellyfish in the Mediterranean Sea. *Zootaxa* **3794**, 455–468. doi:10.11646/zootaxa.3794.3.7

Rambaut, A. (2006). FigTree: Tree Figure Drawing Tool, Version 1.2.2. Institute of Evolutionary Biology, University of Edinburgh. Available at http://tree.bio.ed.ac.uk/software/figtree/ [Accessed 7 June 2015]

Rambaut, A., Suchard, M. A., Xie, D., and Drummond, A. J. (2014). Tracer v1.6. Available at http://beast.bio.ed.ac.uk/Tracer

Ramšak, A., Stopar, K., and Malej, A. (2012). Comparative phylogeography of meroplanktonic species, *Aurelia* spp. and *Rhizostoma pulmo* (Cnidaria: Scyphozoa) in European Seas. *Hydrobiologia* **690**, 69–80. doi:10.1007/s10750-012-1053-9

Ronquist, F., and Huelsenbeck, J. P. (2003). MRBAYES 3: Bayesian phylogenetic inference under mixed models. *Bioinformatics* **19**, 1572–1574. doi:10.1093/bioinformatics/btg180

Rottini Sandrini, L., and Avian, M. (1991). Reproduction of *Pelagia noctiluca* in the central and northern Adriatic Sea. *Hydrobiologia* **216–217**, 197–202. doi:10.1007/BF00026462

Rottini Sandrini, L., Bratina, F., and Avian, M. (1986). Aspetti ultrastrutturali della gametogenesi in *Discomedusa lobata* (Claus). *Nova Thalassia* **8**, 59–66.

Russell, F. S. (1970). 'The Medusae of the British Isles. II. Pelagic Scyphozoa, with a Supplement to the First Volume on Hydromedusae.' (Cambridge University Press: Cambridge, UK.)

Schroth, W., Jarms, G., Streit, B., and Schierwater, B. (2002). Speciation and phylogeography in the cosmopolitan marine moon jelly, *Aurelia* sp. *BMC Evolutionary Biology* **2**, 1–10. doi:10.1186/1471-2148-2-1

Simon, C., Franke, A., and Martin, A. (1991). The polymerase chain reaction: DNA extraction and amplification. In 'Molecular Techniques

in Taxonomy'. (Eds G. M. Hewitt, A. W. B. Johnson and J. P. W. Young.) pp. 329–355. (Springer Verlag: Berlin.)

Sonnenberg, R., Nolte, A. W., and Tautz, D. (2007). An evaluation of LSU rDNA D1–D2 sequences for their use in species identification. *Frontiers in Zoology* **4**, 6. doi:10.1186/1742-9994-4-6

Stamatakis, A. (2014). RAxML Version 8: a tool for phylogenetic analysis and post-analysis of large phylogenies. *Bioinformatics*. doi:10.1093/bioinformatics/btu033

Stopar, K., Ramšak, A., Trontelj, P., and Malej, A. (2010). Lack of genetic structure in the jellyfish *Pelagia noctiluca* (Cnidaria: Scyphozoa: Semaeostomeae) across European seas. *Molecular Phylogenetics and Evolution* **57**, 417–428. doi:10.1016/j.ympev.2010.07.004

Tamura, K., Stecher, G., Peterson, D., Filipski, A., and Kumar, S. (2013). MEGA6: Molecular Evolutionary Genetics Analysis Version 6.0. *Molecular Biology and Evolution* **30**, 2725–2729. doi:10.1093/molbev/mst197

Vanhöffen, E. (1902). Die Acraspeden Medusen der deutschen Tiefsee-Expedition 1898–1899. Deutsche Tiefsee-Expedition 1898–1899, **3**, 1–52, pl 1–8.

Verheyen, E., Salzburger, W., Snoeks, J., and Meyer, A. (2003). Origin of the superflock of cichlid fishes from Lake Victoria, East Africa. *Science* **300**, 325–329. doi:10.1126/science.1080699

Verovnik, R., Sket, B., and Trontelj, P. (2005). The colonization of Europe by the freshwater crustacean *Asellus aquaticus* (Crustacea: Isopoda) proceeded from ancient refugia and was directed by habitat connectivity. *Molecular Ecology* **14**, 4355–4369. doi:10.1111/j.1365-294X.2005.02745.x

Watson, G. M., and Wood, R. L. (1988). Colloquium on terminology. In 'The Biology of Nematocysts'. (Eds D. A. Hessinger and H. M. Lenhoff.) pp. 21–23. (Academic Press: San Diego, CA.)

White, T. J., Bruns, T., Lee, S., and Taylor, J. (1990). Amplification and direct sequencing of fungal ribosomal RNA genes for phylogenetics. In 'PCR Protocols'. (Eds M. A. Innis., G. H. Gelfand, J. J. Sninsky and T. J. White.) pp. 315–332. (Academic Press: San Diego, CA.)

Widersten, B. (1965). Genital organs and fertilization in some Scyphozoa. *Zoologiska Bidrag Uppsala* **37**, 45–58.

Xia, X., Xie, Z., Salemi, M., Chen, L., and Wang, Y. (2003). An index of substitution saturation and its application. *Molecular Phylogenetics and Evolution* **26**, 1–7. doi:10.1016/S1055-7903(02)00326-3

Zakšek, V., Sket, B., and Trontelj, P. (2007). Phylogeny of the cave shrimp *Troglocaris*: evidence of a young connection between Balkans and Caucasus. *Molecular Phylogenetics and Evolution* **42**, 223–235. doi:10.1016/j.ympev.2006.07.009